Chemical enrichment of giant planets and discs due to pebble drift

Richard A. Booth,[★] Cathie J. Clarke, Nikku Madhusudhan and John D. Ilee

Institute of Astronomy, University of Cambridge, Madingley Road, Cambridge CB3 0HA, UK

ABSTRACT

Chemical compositions of giant planets provide a means to constrain how and where they form. Traditionally, super-stellar elemental abundances in giant planets were thought to be possible due to accretion of metal-rich solids. Such enrichments are accompanied by oxygen-rich compositions (i.e. C/O below the disc's value, assumed to be solar, C/O = 0.54). Without solid accretion, the planets are expected to have sub-solar metallicity, but high C/O ratios. This arises because the solids are dominated by oxygen-rich species, e.g. H_2O and CO_2, which freeze out in the disc earlier than CO, leaving the gas metal poor but carbon rich. Here we demonstrate that super-solar metallicities can be achieved by gas accretion alone when growth and radial drift of pebbles are considered in protoplanetary discs. Through this mechanism, planets may simultaneously acquire super-solar metallicities and super-solar C/O ratios. This happens because the pebbles transport volatile species inwards as they migrate through the disc, enriching the gas at snow lines where the volatiles sublimate. Furthermore, the planet's composition can be used to constrain where it formed. Since high C/H and C/O ratios cannot be created by accreting solids, it may be possible to distinguish between formation via pebble accretion and planetesimal accretion by the level of solid enrichment. Finally, we expect that Jupiter's C/O ratio should be near or above solar if its enhanced carbon abundance came through accreting metal-rich gas. Thus, *Juno*'s measurement of Jupiter's C/O ratio should determine whether Jupiter accreted its metals from carbon-rich gas or oxygen-rich solids.

Key words: planets and satellites: atmospheres – planets and satellites: composition – planets and satellites: formation – planets and satellites: individual: Jupiter – protoplanetary discs.

1 INTRODUCTION

The chemical compositions of giant planets can provide insights into how they formed due to variations in the chemical composition of their host discs (Öberg, Murray-Clay & Bergin 2011; Madhusudhan, Amin & Kennedy 2014b; Cridland, Pudritz & Alessi 2016; Eistrup, Walsh & van Dishoeck 2016; Madhusudhan et al. 2016; Ali-Dib 2017). One key aspect is how and where they accreted their metals, because the abundance ratios such as C/N or C/O are correlated with their absolute abundances with respect to hydrogen in a way that depends on where the planet formed. In particular, because oxygen-rich species such as H_2O and CO_2 freeze out at higher temperatures than CO, the dust grains in protoplanetary discs always have sub-solar C/O ratios, leaving the gas super-solar in C/O. Thus, measurements of the C/O ratio provide a way of determining whether the planet accreted its metals predominantly by accreting gas or solids in the form of dust grains or planetesimals.

Since planet formation theories make differing predictions about when and how much solids are accreted, chemical constraints on the amount of solids accreted are able to place constraints on how the planets formed too. For example, giant planets that form through the gravitational instability are thought to form early (Boss 2000; Clarke & Lodato 2009; Rice & Armitage 2009; Boley & Durisen 2010; Forgan & Rice 2011). Since the initial accretion of gas and solids should be equally efficient for planets formed by the gravitational instability, they will acquire similar compositions to their host stars as there is little time for chemical processing in the disc. However, in core accretion, giant planets must first grow 10–20 $M_\oplus$ rocky cores before accreting their gaseous envelopes. The classical model for core formation by runaway planetesimal collisions typically requires several Myr (Pollack et al. 1996; Kobayashi, Tanaka & Krivov 2011), which is long compared with the disc's lifetime (a few Myr; Haisch, Lada & Lada 2001; Currie et al. 2009; Fedele et al. 2010; Meng et al. 2017). Eventually, the planets undergo runaway accretion of gas and rapidly accrete their gaseous envelopes, but not until after significant chemical processing may have occurred in the disc (Eistrup et al. 2016).

Recently, a variant of the standard core accretion model, known as pebble accretion, has been shown to overcome the growth time-scale problem, producing the cores of giant planets within ∼10^5 yr (Ormel & Klahr 2010; Lambrechts & Johansen 2012). In this model,

★ E-mail: rab200@ast.cam.ac.uk

planetary embryos grow by accreting mm- or cm-sized pebbles from a gas-rich disc. Observations of protoplanetary discs show that there is a reservoir of such pebbles from which the embryos can accrete (Wilner et al. 2005; Rodmann et al. 2006; Lommen et al. 2007; Pérez et al. 2012; Tazzari et al. 2016), making pebble accretion an attractive model for the formation of giant planets.

One important difference between the standard planetesimal accretion scenario and pebble accretion is in the prospects for the late accretion of solids. Once the planetary cores become massive enough to perturb the gas surface density in the disc, the flux of pebbles from the outer disc is trapped in a pressure maximum outside the planet's orbit and pebble accretion stops (Lambrechts, Johansen & Morbidelli 2014; Rosotti et al. 2016). The planet then slowly accretes gas as the envelope contracts until eventually runaway gas accretion occurs. Without the presence of planetesimals, this results in a relatively clean envelope that has not been enriched by solids. Conversely, in the planetesimal accretion scenario, the accretion of solids continues during the envelope contraction phase (Pollack et al. 1996), and may continue subsequently until the planet's feeding zone becomes depleted in planetesimals (e.g. Alibert et al. 2005), possibly leading to highly enriched atmospheres. We note that in practice there is likely to be some middle ground between these two extremes (e.g. the presence of some planetesimals even if the cores form by pebble accretion so it is not clear how much enhancement to expect). The enrichment of planetary atmospheres is further complicated by whether the planetesimals are disrupted in the envelope or reach the core (Mordasini et al. 2015; Pinhas, Madhusudhan & Clarke 2016), along with the possibility that the planet's core may be partially eroded and mixed throughout the envelope (Wilson & Militzer 2012).

With the robust detection of molecular species such as H_2O, CH_4, CO and CO_2 becoming possible in the atmospheres of hot Jupiters, the idea of testing planet formation using planet composition is very appealing (Lodders & Fegley 2002; Madhusudhan 2012; Moses et al. 2013; Tsai et al. 2017). In particular, the water abundance in the spectrum of a hot Jupiter provides a strong constraint on the C/O ratio: if the observed water abundance is far below that expected for the stellar C/O ratio, then one can infer that the C/O ratio is close to unity (Madhusudhan 2012), modulo any possible uncertainty due to obscuration of the water feature by clouds or hazes (see Madhusudhan et al. 2016, and references therein, for a recent discussion). Nevertheless, observations show that hot Jupiters may have C/O ratios that range from approximately stellar (Kreidberg et al. 2014; Line et al. 2014; Haynes et al. 2015) to C/O $\gtrsim$ 1 (Madhusudhan et al. 2011; Stevenson et al. 2014).[1]

The Solar system giant planets provide another opportunity to probe planet formation. Models can place constraints on their location during terrestrial planet formation, requiring them to be near their current locations during the process (e.g. Tsiganis et al. 2005; Raymond, Quinn & Lunine 2006; Walsh et al. 2011; Agnor & Lin 2012; Raymond et al. 2014). This suggests that they either formed *in situ* or migrated through the disc. Other 'disc-free' modes of migration such as planet–planet scattering or the Kozai–Lidov mechanism (Kozai 1962; Lidov 1962) can be ruled out, due to the giant planets' low eccentricities. Furthermore, the lack of a suitable

companion and the long time required also disfavour the Kozai–Lidov mechanism.

While we know that Jupiter is carbon rich, with a C/H ratio approximately three to five times solar, and is also enriched in noble gases, along with nitrogen and sulphur (Owen et al. 1999; Atreya & Wong 2005), currently the oxygen abundance is uncertain. Saturn's abundances are in general more uncertain, but the C/H ratio is well determined to be about eight times solar and the N/H ratio is around three times solar (Atreya et al. 2016). Although the oxygen abundance remains uncertain for both Jupiter and Saturn, the Galileo probe's measurement of water in a hotspot in Jupiter's atmosphere provides a possible constraint (Owen et al. 1999; Atreya & Wong 2005; Atreya et al. 2016). Galileo found an O/H ratio of about one half solar, giving a C/O ≈ 10, but it is not clear that the measurement is representative of Jupiter's bulk atmosphere. Using thermochemical models, Visscher, Moses & Saslow (2010) were able to place a lower limit on the C/O ratio, suggesting that C/O ratios that are less than about half solar (C/O $\lesssim$ 0.25) are incompatible with the levels of CO detected in Jupiter's atmosphere. However, the *Juno* satellite should soon provide us with a reliable measurement of water in Jupiter (Matousek 2007), which can be used to determine the global O/H ratio (Helled & Lunine 2014). The imminent availability of *Juno*'s measurement of Jupiter's water abundance provides us with an excellent opportunity to constrain the formation of giant planets.

A super-solar C/O ratio along with a high C/H for Jupiter is in tension with current models of planet formation, which generally predict that planets with super-solar C/H ratios should normally have sub-solar C/O ratios (Öberg et al. 2011; Madhusudhan et al. 2014b, 2016; Cridland et al. 2016; Eistrup et al. 2016; Ali-Dib 2017). The sub-solar C/O ratios arise because the additional carbon is brought into the planet's envelope by accreting *solids* (either in the form of planetesimals or by partially eroding the core) because the condensation of volatile species results in a depleted gas phase carbon abundance. Since H_2O and CO_2 condense at higher temperatures than CO, the solids are always oxygen rich unless a high fraction (∼50 per cent) of the carbon is locked up into refractory organic molecules. Similarly, the gas ends up with a sub-solar C/H ratio but super-solar C/O ratio. Combining varying amount of gas and solids results in planetary compositions that have either a C/H ratio above solar but a C/O ratio below solar, or a C/O ratio above solar with a C/H ratio below solar. Thus, the compositions of giant planets are restricted to two octants of the C/H versus O/H ratio plane (see e.g. Madhusudhan et al. 2014b, 2016).

The above correlations between predicted elemental ratios arise naturally from partitioning solar composition gas into solids and ices according to condensation temperature of different molecular species. If the C/O ratio in Jupiter turns out to be high, then this can be achieved in one of two ways: (1) change the C/O ratio of the solids accreted, for example by accreting from an as of yet unknown family of organic-rich planetesimals (Lodders 2004) or (2) change the abundance of the gas to make it more carbon rich, such as through photoevaporation (Guillot & Hueso 2006; Monga & Desch 2015).

In this paper, we explore idea (2) and argue that high gas phase C/H and C/O ratios might arise naturally as a consequence of disc evolution. The key point is that the large reservoir of mm- or cm-sized grains are expected to migrate radially. As the grains migrate, they will carry any volatiles frozen on to their surface to snow lines, where the volatiles can desorb enhancing the local chemical abundance. Subsequent advection with the gas and diffusion may then spread these molecules inwards throughout the disc. This idea

---

[1] Throughout this work, we use the solar C/O ratio (≈0.54) as our base value. As noted by Brewer, Fischer & Madhusudhan (2017), when considering exoplanets the reader should bear in mind that the comparison must be made to the stellar abundances, which can be sub-solar.

has been explored in relation to the water snow line or generic volatiles (Stepinski & Valageas 1997; Hueso & Guillot 2003; Ciesla & Cuzzi 2006; Garaud 2007); however, increasing the abundance of water inside the water snow line is clearly of little help in enhancing the C/O ratio. However, the enhancement of CO can increase the CO ratio from its solar value of C/O ≈ 0.54 (Asplund et al. 2009) to nearly twice the solar value, along with the C/H ratio, as suggested by Öberg & Bergin (2016).

The accretion of these metal-rich gases can then directly produce metal-rich planetary envelopes, without the need for subsequent accretion of solids or erosion of the core. Although this way of enhancing the envelope's abundances is independent of the way in which the planet's core is formed, we note that it fits naturally into the pebble accretion model because the pebbles responsible for the rapid accretion are also those that dominate the flux of volatiles. For this reason, we have focused on the pebble accretion model of planet formation, but giant planets with cores that formed by the accretion of planetesimals may also accrete metal-rich gas this way. Indeed, the differences between the chemical abundances produced in our models and those discussed above are more due to the disc evolution model than the planet formation model *per se*.

In Section 2, we describe the global models that we use for the evolution of the gas and grain populations in the disc, for the formation of planets and for disc chemistry. In Section 3, we describe the resulting evolution of the disc, focusing on the evolution of elemental abundances at different locations in the disc. In Section 4.1, the results of the planet formation model are presented, along with the chemical composition of their atmospheres in Section 4.2. In Section 4.3, we discuss our models in the context of the formation of Jupiter and Saturn. In Section 5, we discuss our results in terms of observations of protoplanetary discs and planetary atmospheres. In Section 6, we present our conclusions.

2 MODEL

We base our model for dust evolution on the two-population model of Birnstiel, Klahr & Ercolano (2012), which is ideal for our purposes because it has been calibrated to match the grain size and mass flux in detailed simulations of growth and radial drift. The evolution of the gas is treated using a simple viscous evolution model. The dust is treated by considering two populations of grains: small grains that remain tightly coupled to the gas and large grains that may grow and drift. We have extended the model to include the effects of feedback from the dust on the gas, which can become important in regions of high dust density. Additionally, we follow evolution of the dominant carbon- and oxygen-bearing species, which may be present as varying fractions of vapour and ice. Our treatment for adsorption and desorption of molecular species follows insights from grain growth and chemical models, and agrees well with a detailed study on the delivery of CO to the CO snow line by Stammler et al. (2017).

2.1 Disc evolution

We model the disc evolution, following the viscous evolution of the gas, growth and radial drift of solids, and a simple model for the adsorption and desorption of the dominant carbon- and oxygen-bearing species. The coupled evolution of the dust and gas is solved in a 'one-fluid' manner, following Laibe & Price (2014). This ap-

proach involves solving for the evolution of the total surface density,

$$\Sigma = \Sigma_G + \sum_i \Sigma_{Di}, \tag{1}$$

along with the dust fractions $\epsilon_i = \Sigma_{Di}/\Sigma$. Here Σ_G and Σ_{Di} are the surface density of the gas and the ith dust species. From conservation of mass and momentum, the usual viscous evolution equation (Lynden-Bell & Pringle 1974) can be extended to the multi-fluid case,

$$\frac{\partial \Sigma}{\partial t} = \frac{1}{R} \frac{\partial}{\partial R} \left[3R^{1/2} \frac{\partial}{\partial R} \left(\nu \Sigma_G R^{1/2} \right) \right], \tag{2}$$

where ν is the kinematic viscosity and we have made the usual approximation that the velocity profile does not significantly differ from Keplerian rotation. Additionally, we assume that viscosity only drives angular momentum transport in the gas. We use an α model for the viscosity $\nu = \alpha c_s H$, where c_s is the sound speed and $H = c_s/\Omega$ is the disc scaleheight. The sound speed is calculated from the temperature assuming a mean-molecular weight, $\mu = 2.4$. To compute the temperature, we follow Birnstiel, Dullemond & Brauer (2010) and use the model of Hueso & Guillot (2005), which includes viscous heating, irradiation from a central star and external radiation. For the opacity, we use the updated Bell & Lin (1994)-type tabulated opacity provided by Zhu et al. (2012). For the stellar properties, we use $M = 1\,M_\odot$, $R = 2.5\,R_\odot$ and $T_{eff} = 4200\,K$, while we assume that external irradiation limits the temperature to be at least 10 K.

By noting that the viscous radial velocity, v_R, is given by

$$\Sigma v_R = 3R^{-1/2} \frac{\partial}{\partial R} \left(\nu \Sigma_G R^{1/2} \right), \tag{3}$$

a trace quantity with concentration, ϕ, can be followed by advecting the mass of the tracer $\Sigma \phi$ at velocity v_R,

$$\frac{\partial (\Sigma \phi)}{\partial t} = \frac{1}{R} \frac{\partial}{\partial R} \left[R v_R (\Sigma \phi) \right]. \tag{4}$$

Numerically, we solve equations (2) and (4) using a first-order explicit finite-volume update following Bath & Pringle (1981).

We follow Laibe & Price (2014) for the update of the dust fraction, who give an expression the evolution of ϵ_i in a Lagrangian frame, which we write as

$$\frac{d\epsilon_i}{dt} = \frac{1}{\Sigma R} \frac{\partial}{\partial R} \left[R \Sigma \epsilon_i (\Delta v_i - \epsilon \Delta v) \right]. \tag{5}$$

Here $\Delta v_i = v_i - v_g$, the difference between the dust and gas radial velocity and $\epsilon \Delta v = \sum_i \epsilon_i \Delta v_i$. To compute the relative velocity, we follow Tanaka, Himeno & Ida (2005), who provide an expression for the dust–gas relative velocity of a distribution of grain sizes when feedback is included. An equivalent form is given by Bai & Stone (2010). The radial component of the relative velocity is given by

$$\Delta v_i = \frac{2v_\phi St_i - v_r St_i^2}{1 + St_i^2}, \tag{6}$$

where v_r and v_ϕ are the radial and azimuthal velocity of the gas,

$$v_r = -\frac{1}{\rho_G \Omega} \frac{dP}{dR} \frac{\lambda_1}{(1 + \lambda_0)^2 + \lambda_1^2}, \tag{7}$$

$$v_\phi = \frac{1}{2} \frac{1}{\rho_G \Omega} \frac{dP}{dR} \frac{1 + \lambda_0}{(1 + \lambda_0)^2 + \lambda_1^2}. \tag{8}$$

Here, the mid-plane values of the pressure, P, and gas density, ρ_G, are used and

$$\lambda_k = \sum_i \left(\frac{\epsilon_i}{1 - \epsilon} \right) \left(\frac{St_i^k}{1 + St_i^2} \right). \tag{9}$$

The Stokes number, $St_i = \frac{\pi}{2} \rho_s s_i / \Sigma_G$, i.e. assuming Epstein drag for spherical grains in the disc mid-plane, where $\rho_s = 1\,\mathrm{g\,cm^{-3}}$ is the internal density of the grain and s_i is its radius. In the complete update of ϵ_i, we first advect ϵ_i as a tracer in the viscous evolution step. Then we compute Δv_i using centred finite differences and use an explicit upwind finite-volume update for equation (5). Trace species that move with the dust, such as ices, are advected analogously to those moving with the gas.

Additionally, we include the diffusion of dust and trace species given by

$$\frac{\partial \phi}{\partial t} = \frac{1}{R \Sigma} \frac{\partial}{\partial R} \left[R D_\phi \Sigma \frac{\partial \phi}{\partial R} \right], \tag{10}$$

where $D_\phi = \nu / Sc_\phi$, where Sc_ϕ is the Schmidt number of the tracer. For gas tracers, we take $Sc_\phi = 1$, while for dust we use $\phi_i = \epsilon_i$ and

$$Sc_i = \frac{(1 + St_i^2)^2}{1 + 4St_i^2} \tag{11}$$

(Youdin & Lithwick 2007). This diffusive flux is included as an extra term in equation (5).

2.2 Grain growth

For grain growth, we follow the prescription given in appendix B of Birnstiel et al. (2012). In this model, the large grains grow on a time-scale, $t_{grow} = (\epsilon \Omega)^{-1}$, until their growth is prevented by radial drift or fragmentation. In the outer parts of the disc, grain growth is limited as the radial drift time-scale becomes shorter than the growth time-scale and thus the grains are removed before they can grow. This occurs at a Stokes number,

$$St_{drift} = 0.55 \epsilon \left(\frac{R}{H} \right)^2 \left| \frac{d \ln P}{d \ln R} \right|^{-1}. \tag{12}$$

At smaller radii, growth is eventually limited by fragmentation driven by the turbulent velocities of dust grains, limiting their size to

$$St_{frag} = 0.37 \frac{1}{3\alpha} \frac{v_f^2}{c_s^2}, \tag{13}$$

where v_f is the threshold velocity for fragmentation.

The grains' initial size is taken to be $0.1\,\mu m$. The mass fraction of grains in the large and small populations depends on whether their size is limited by fragmentation or radial drift: if fragmentation limits their growth, then 75 per cent of the mass is in large grains, while the fraction of large grains is 97 per cent if radial drift dominates.

Fragmentation occurs when grains collide at a velocity above their fragmentation threshold, v_f. For icy grains, we take $v_f = 10\,\mathrm{m\,s^{-1}}$ (Gundlach & Blum 2015), while for 'dry' grains we use the fragmentation threshold for silicates, $v_f = 1\,\mathrm{m\,s^{-1}}$ (Blum & Wurm 2008). To determine whether grains are icy or ice-free, we compare the total mass in all of the ices on the grains to the mass of the grains themselves. If this is above 10 per cent, we use the icy fragmentation threshold. For ice concentrations below 10 per cent, we interpolate between the upper and lower thresholds. This choice ensures that the transition between icy and ice-free grains follows the water snow line as the disc evolves.

2.3 Chemistry

We use the simple chemical models of Madhusudhan et al. (2014b), which include only the dominant carbon- and oxygen-bearing volatile species, H_2O, CO, CO_2, CH_4 (Öberg et al. 2011; Madhusudhan et al. 2014b). In Madhusudhan et al. (2014b, 2016), two different models for the abundance fractions of these species were used, Cases 1 and 2, shown in Table 1. These abundance fractions are motivated by either theoretical chemical calculations (Case 1; Woitke, Kamp & Thi 2009) or observation of ice grains in protoplanetary discs (Case 2; Draine 2003; Pontoppidan 2006; Öberg et al. 2011).

In previous studies (Madhusudhan et al. 2014b, 2016), the molecular species were assumed to be entirely in either the gas phase or in ices on the surface of grains, depending on whether the local temperature exceeded some typical condensation temperature. However, such a sharp transition in the chemical abundance results in numerical difficulties because the diffusion of chemical species depends

Table 1. Binding energies and volume mixing ratios of chemical species in the model disc (adapted from Madhusudhan et al. 2014b, 2016).

Species (X)	T_{bind} (K)[a]	Case 1[b]: X/H	Case 2[c]: X/H
CO	850	$0.45\,(1 + f_{CO_2}) \times$ C/H	$0.65 \times$ C/H
CH_4	1300	$0.45\,(1 - f_{CO_2}) \times$ C/H	0
CO_2	2575	$0.1 \times$ C/H	$0.15 \times$ C/H
H_2O	5700	O/H $- (3 \times$ Si/H $+$ CO/H $+ 2 \times CO_2$/H)	O/H $- (3 \times$ Si/H $+$ CO/H $+ 2 \times CO_2$/H)
Carbon grains	–	0	$0.2 \times$ C/H
Silicates	–	Si/H	Si/H

Notes. [a]The binding energies are adopted from Collings et al. (2004), Garrod & Herbst (2006) and Fayolle et al. (2016), and produce ice lines at temperatures of 20, 71 and 180 K for CO, CO_2 and H_2O, respectively. We use the binding energy of pure CO, rather than the higher binding energy of a mixture of CO and water ice. This produces a freeze-out temperature closer to the 20 K used previously.
[b,c]Volume mixing ratios (i.e. by number) adopted for the species as a function of disc elemental abundances under two different prescriptions for condensate chemistry (see e.g. Madhusudhan et al. 2014b). Solar values are assumed for the elemental abundances C/H, O/H and Si/H (Asplund et al. 2009). The Case 2 chemistry is adopted from Öberg et al. (2011) and contains carbon grains leading to more solid carbon. The fraction of CO_2 molecules in ices is denoted by f_{CO_2}.

on their concentration gradient (equation 10), which would not be well defined. Instead, we solve for the equilibrium ice abundance by balancing the thermal adsorption and desorption rates in the mid-plane.

Following Hollenbach et al. (2009) and Visser (2009), the thermal desorption rate *per grain* is given by $4\pi s_0^2 N_{s,i} R_{d,i} f_{s,i}$, where $N_{s,i} = 1.5 \times 10^{15}$ cm^{-2} is the number of binding sites per unit area on the grain, where we have assumed spherical grains and s_0 is their mean size by area. $f_{s,i}$ is the fraction of binding sites covered by the molecule. The desorption rate per molecule is

$$R_{d,i} = 1.6 \times 10^{11} \sqrt{\frac{T_{\mathrm{bind},i}}{\mu_i}} \exp\left(-T_{\mathrm{bind},i}/T\right), \tag{14}$$

where $T_{\mathrm{bind},i}$ and μ_i are the binding energy and mean-molecular weight of the molecule. The binding energies used are given in Table 1. For thermal adsorption, we assume that all molecule–grain collisions result in sticking. Thus, the adsorption rate per grain is given by $n_i \pi s_0^2 v_i$, where n_i is the gas phase number density of the molecule and v_i is its thermal velocity. For the mean grain area, we assume 0.1 μm spherical grains. We note that although the dust mass is dominated by large grains, the surface area of the grains is dominated by small grains for both protoplanetary disc dust populations (Birnstiel, Ormel & Dullemond 2011) and the interstellar medium distribution of grain sizes (Mathis, Rumpl & Nordsieck 1977).[2]

Grain creation or destruction processes have been neglected in the models, i.e. although the grain size may change, the amount of silicate or carbon in grains only changes due to advection and diffusion. The ice mass has been included in ϵ_i when computing the growth and dynamics. We have also compared our equilibrium adsorption–desorption model to models in which we treat these adsorption and desorption processes in a time-dependent manner and find no significant differences, because typically the adsorption time-scale is shorter than the radial drift time-scale, except in the extreme outer parts of the disc.

In all models, we use one of the abundance distributions given in Table 1 for the initial conditions. However, as the disc evolves, the abundances of the molecular species will change due to radial drift. These changes will drive the chemical abundances out of equilibrium and thus we might expect that subsequently chemical reactions would further modify the molecular abundances. We take a simplistic approach and try to capture the important behaviour instead of attempting to model all of the required chemical processes in detail, which would obscure our main focus of investigating the redistribution of molecular species. One way of achieving this is to view the abundances in Table 1 as models of the equilibrium chemical abundances, which chemical processes act to restore. We note that the equilibrium molecular abundances are likely to be dependent on the location in the disc, but for simplicity we neglect any such differences beyond those already included in Table 1.

We consider models that should bracket the possible behaviours by considering two scenarios: one in which reactions are assumed to be negligibly slow and are neglected and one in which the 'equilibrium' abundances of Table 1 are immediately restored. In the first

model, the type of molecule in which each atom is contained always remains the same, though it may adsorb, desorb, advect and diffuse through the disc, thus changing the local abundances. In the second model, the molecules' abundances will additionally change through the conversion of one species into another close to the snow lines. We update the abundances of both the gas and ice phase molecular species, but assume that the amount of material locked up in carbon grains or silicates does not change. We note that due to strong enhancements of CO near its snow line the conversion of CO to CO_2 may require more oxygen than is available. If this is the case, then we create as much CO_2 as possible based on the available oxygen, leave the reaming excess carbon as CO and set the H_2O abundance to zero.

For the Case 1 chemistry, we have only considered the equilibrium abundance model since the CO and CH_4 abundance changes at the CO_2 snow line. Hence, it is not clear that a slow reaction model makes sense for this chemical abundance pattern. Furthermore, since the fraction of CO_2 in ices now varies smoothly across the snow line, we replace the sharp transition in the CO and CH_4 abundances with one smoothed by interpolating between the two regimes based upon the fraction of CO_2 in the gas phase.

In reality, the effect of chemical reactions will lie between these two extremes of our models. Eistrup et al. (2016) show that the time-scale for the formation and destruction of the molecular species we consider typically occurs on time-scales of around a few 10^5 yr. This time-scale falls between the radial drift time-scale (a few 10^4 yr) and the time-scale for viscous evolution and gas diffusion ($\sim$Myr). We can have some confidence that our models will capture the qualitative behaviour because the detailed chemical models of Eistrup et al. (2016) produce similar abundance patterns to our Case 1 chemical model when starting from the molecular abundances inherited from the parent cloud.

2.4 Planet formation

We focus on giant planet formation by pebble accretion. For this, we use the model based on Bitsch, Lambrechts & Johansen (2015), which we only describe briefly. The only significant difference between our planetary growth model and the Bitsch et al. (2015) model is the way that we determine the surface density and size of the pebbles used in the pebble accretion model. We use directly the values obtained from our disc evolution models, while Bitsch et al. (2015) use the prescriptions of Lambrechts & Johansen (2014). However, since the Lambrechts & Johansen (2014) model is also based upon insights from grain growth models, such as the Birnstiel et al. (2012) model that we use, we do not expect the differences to be too great.

Pebble accretion stops once the planet is massive enough to open a gap in the pebbles, which occurs when

$$M_{\mathrm{p}} \approx 20 \left(\frac{H/R}{0.05}\right)^3 M_\oplus \tag{15}$$

(Lambrechts et al. 2014; Rosotti et al. 2016). Initially, the gas accretion rate is slow and is controlled by envelope contraction. During this phase, we follow Piso & Youdin (2014) and the planet's envelope grows according to

$$\dot{M}_{\mathrm{env}} = 1.75 \times 10^{-3} f^{-2} \left(\frac{\kappa_{\mathrm{env}}}{1\,\mathrm{cm}^2\,\mathrm{g}^{-1}}\right)^{-1} \left(\frac{\rho_{\mathrm{c}}}{5.5\,\mathrm{g}\,\mathrm{cm}^{-3}}\right)^{-1/6}$$

$$\times \left(\frac{M_{\mathrm{c}}}{M_\oplus}\right)^{11/3} \left(\frac{M_{\mathrm{env}}}{0.1\,M_\oplus}\right)^{-1} \left(\frac{T}{81\,\mathrm{K}}\right)^{-1/2} M_\oplus\,\mathrm{Myr}^{-1}, \tag{16}$$

---

[2] Although it may appear surprising, using simulations including the full grain size distribution Stammler et al. (2017) showed that the adsorption on to small grains is indeed the dominant contribution to the adsorption rate of molecules but that the large grains contain the most of the mass in ices and dominate the radial flux of ices. Our simplified model captures these behaviours.

where M_c is the core mass, $\kappa_{\rm env} = 0.05\,{\rm cm^2\,g^{-1}}$ is the opacity of the envelope, $\rho_c = 5.5\,{\rm g\,cm^{-3}}$ is the core's density and the factor $f = 0.2$ (see Bitsch et al. 2015, for a discussion of these parameters). The planet's accretion rate during the envelope contraction only depends on the disc's properties through its local temperature, T. Once the envelope becomes as massive as the core, runaway gas accretion occurs. We use the accretion rate from Machida et al. (2010), with a maximum gas accretion rate limited to 80 per cent of the disc accretion rate.

We have not included any late-phase pebble or planetesimal accretion, which would further enrich the envelope (Mordasini et al. 2015; Pinhas et al. 2016). We follow the chemical composition of the planets by tracking separately the mass accreted in solids and gas, along with the composition of those components. In this way, we build up the total composition of the core and envelope of the planet. Subsequent erosion of the core may mix some of the solids into the envelope.

Planetary migration is also included following Bitsch et al. (2015). For Type I migration, we use the torque formulae of Paardekooper, Baruteau & Kley (2011), while for Type II migration use the results of Baruteau et al. (2014). We interpolate between these limits using the gap opening criterion of Crida & Morbidelli (2007). Once the planets migrate close to the inner edge of the simulation, we stop tracking their growth and migration.

We note that the feedback of the planets on the disc has not been included: we have neglected the changes in disc mass due to planetary accretion or the surface density due to the torque from the planet.

2.5 Initial conditions

We set up the disc with an the initial surface density given by

$$\Sigma(R) = \frac{\dot{M}}{3\pi\nu}\exp\left(-R/R_d\right), \tag{17}$$

and we typically use $\dot{M} = 10^{-8}\,{\rm M_\odot\,yr^{-1}}$, $R_d = 100$ and $\alpha = 10^{-3}$ unless otherwise stated. Since ν depends on Σ because the temperature depends on the optical depth, we iterate the initial surface density until ν and Σ converge. We assume that the atomic abundances are initially solar (Asplund et al. 2009) and the molecular

abundances are given by either the Case 1 or Case 2 values. The dust mass is set to the sum of the carbon grains, silicate grains and any molecules that have condensed into ices according to Table 1. In Fig. 1, we show the initial dust fraction and abundances for the two models. This figure shows clearly why models of planet formation without disc evolution predict that Jupiter must have a C/O ratio that is at most solar: Jupiter's high C/H ratio means that these model planets must have accreted their additional carbon in the form of solids, which are typically oxygen rich.

3 CHEMICAL EVOLUTION OF THE DISC

3.1 No or negligibly slow reactions

We first consider the evolution of the disc and chemistry for the model in which the chemical reactions are assumed to be slow, using the Case 2 abundances. Initially, the total gas+ice composition of each molecule is the same everywhere. Fig. 2 shows the evolution of the fiducial disc model. The growth and radial drift of the grains cause the outer disc to become depleted of dust after about a Myr. Beyond 10 au, the size of the grains is limited by radial drift; thus, the maximum size of the dust grains also decreases due to the slower growth rate at lower dust-to-gas ratios. In the inner regions, fragmentation limits grain growth and the maximum grain size does not evolve. The transition from icy to bare grains at the water snow line reduces the fragmentation threshold, resulting in smaller grains, lower radial drift speeds and higher dust fractions.

The radial drift of grains from the outer disc carries CO, CO_2 and H_2O ices towards the star. As grains cross their corresponding snow lines, the volatiles evaporate. Since the grains drift faster than the volatiles diffuse, this produces local spikes in the concentrations of molecular species near their snow lines. Inside the CO snow line, CO_2 and H_2O continue to be carried towards the star by radial drift until the molecules meet their own snow lines. Thus, the gas becomes enriched in CO just inside the CO snow line, but becomes depleted in CO_2 and H_2O as they are carried into the inner disc along with the dust grains. This results in the carbon and oxygen abundance becoming dominated by the gas phase CO inside the CO snow line, CO_2 inside the CO_2 snow line and H_2O close to the star. Hence, between the CO and CO_2 snow line, the disc ends
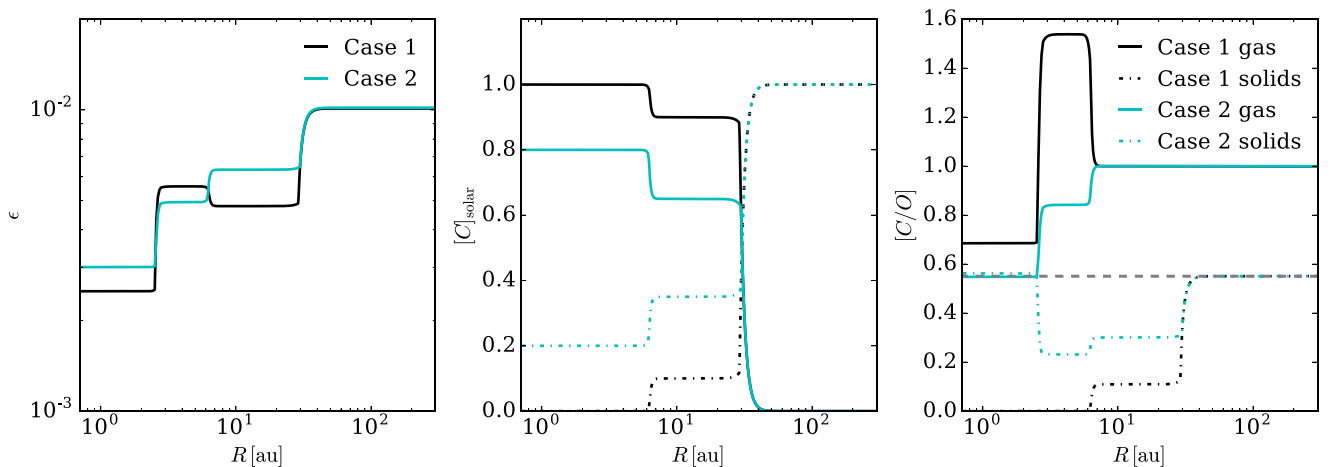

Figure 1. Initial dust-to-gas ratio (left), carbon abundance (centre) and C/O ratio (right) for the two chemical models. The grey dashed line in the right-hand panel shows the solar C/O ratio. The C/O ratio in the gas phase is always super-solar, but the gas phase carbon abundance is sub-solar. Note that the carbon abundance in the middle panel is normalized by the total dust + gas mass for both the gaseous and solid carbon.
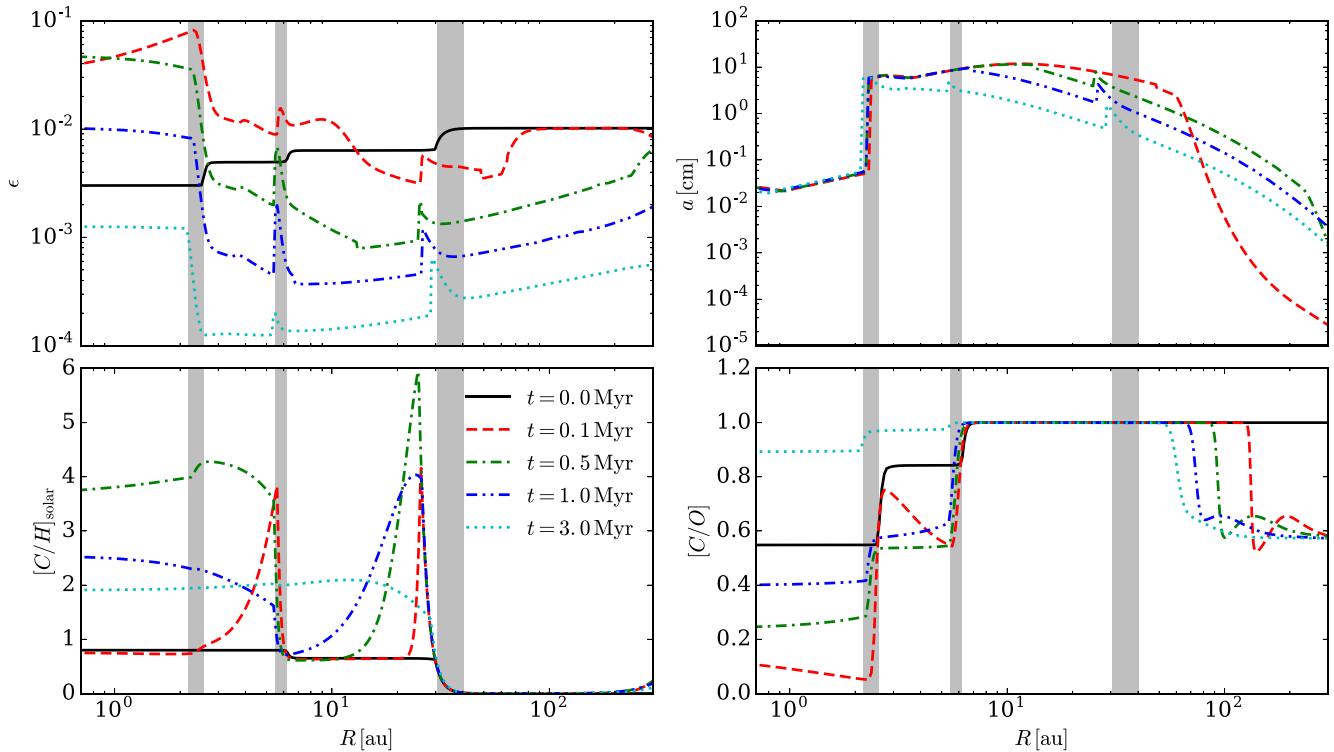
Figure 2. Evolution of the dust fraction (top left), grain size (top right), gas phase carbon abundance relative to the solar abundance (bottom left) and gas phase C/O ratio (bottom right) for the Case 2 chemistry model. The jump in grain size at the water snow line (located at a few au) is due to the lower threshold velocity for fragmentation for non-icy grains. The grey bars show the regions where the H_2O, CO_2 and CO snow lines are located (from left to right, respectively).

up with high C/H ratios and C/O = 1. Closer to the star, the C/O ratio decreases because the C/O ratio of the volatiles released at the subsequent ice lines decreases, with the C/O ratio becoming sub-solar in the inner disc despite the high C/H ratio. As a consequence of the radial transport, the disc beyond the CO snow line becomes sub-solar in composition.

Eventually, the flux of dust grains and ices from the outer disc decreases and the disc's evolution is then dominated by the viscous evolution of the gas and diffusion of the molecular species. Since the disc evolves most rapidly at small radii, the water-rich gas in the inner disc is accreted before the CO- and CO_2-rich gas further out. Thus, as the disc continues to evolve, the C/O ratio in the inner disc increases as the disc becomes increasingly dominated by CO.

As a further illustration, Fig. 3 shows the abundances of the gas and ice phase molecular species at 0.5 Myr relative to their initial total (gas + ice) abundance. This figure demonstrates that typically a single species is responsible for the gas phase abundance, except inside the water snow line where the abundance of both H_2O and CO_2 is high. We also see that the ice composition of the dust grains only changes close to snow lines, with the change in abundance relative to the initial abundance arising due to the change in dust-to-gas ratio.

3.2 Fast reactions: equilibrium abundances

The model in the previous section examines how the radial drift of dust grains can redistribute volatiles in the disc when chemical processes occur much more slowly than radial drift. In that case, the volatiles are transported rapidly to their ice lines, where they evaporate and are left behind. This leads to large concentrations of

particular species close to the ice lines and thus chemical distributions that are out of equilibrium.

These large imbalances in chemical species may drive chemical reactions. If these reactions occur rapidly enough, they may drive the chemical abundances back to a new equilibrium. We investigate the effects that such fast reactions may have on the redistribution of volatiles in a model where the molecular abundances are set back to their equilibrium values based on Table 1. We note that this neglects that different equilibria are possible at different temperatures and compositions; however, it can demonstrate how chemical reactions may affect the redistribution process.

In Fig. 3, we show the molecular abundances of this equilibrium chemistry model, while Fig. 4 shows the evolution. Although the grain size and dust-to-gas ratio evolution is nearly identical to the slow reaction model, the chemical abundances differ significantly. Notably, the carbon abundance is decreased near the CO snow line relative to the no reaction model, while it is increased inwards from the CO_2 snow line.

The higher carbon abundance at the CO_2 snow line in the equilibrium model can be understood in terms of an extra transport mechanism for CO. In the no reaction model, CO can only move inwards of the CO snow line by diffusion and gas phase advection. However, in the equilibrium reaction model, some of the CO is converted to CO_2, reducing the carbon abundance with respect to the no reaction model. This CO_2 then freezes out and is transported inwards along with the grains. This produces an overabundance of CO_2, some of which is converted back to CO, enhancing the CO and water ice abundances between the CO and CO_2 snow lines.

The efficiency of the CO_2 ice production and transport depends on the supply of oxygen (in the form of water in our models), required for the conversion of CO into CO_2. Within $\sim 10^5$ yr, the
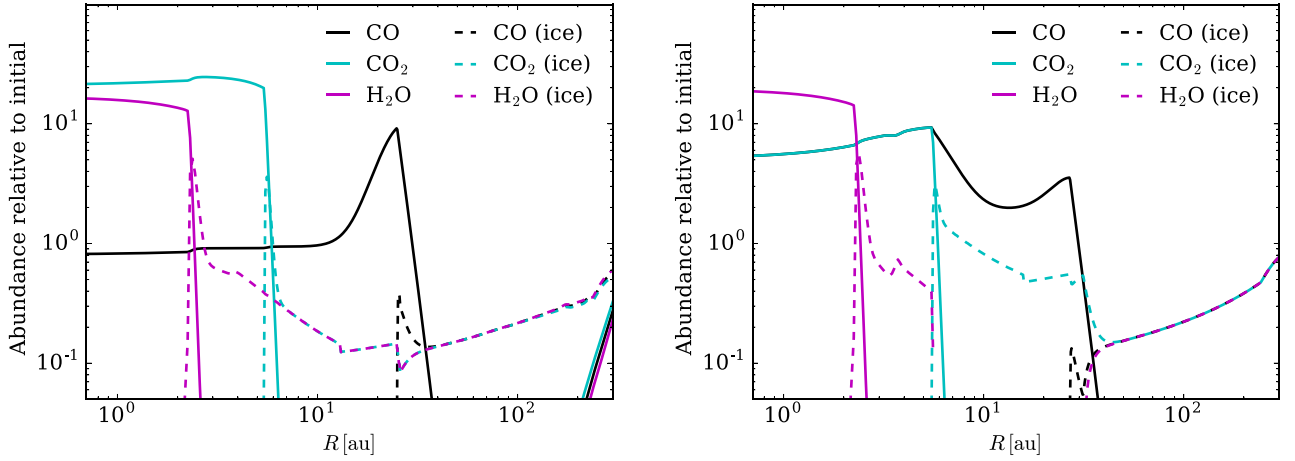
Figure 3. Abundance of the main carbon and oxygen carriers relative to their initial abundance at 0.5 Myr. These abundances are calculated using the Case 2 chemical model under the assumption that chemical reactions can be neglected (left) or that equilibrium abundances are maintained (right). In the right-hand panel, the lines showing the relative abundance of CO and CO_2 in the gas lie on top of each other inside of the CO_2 snow line at 5–6 au.
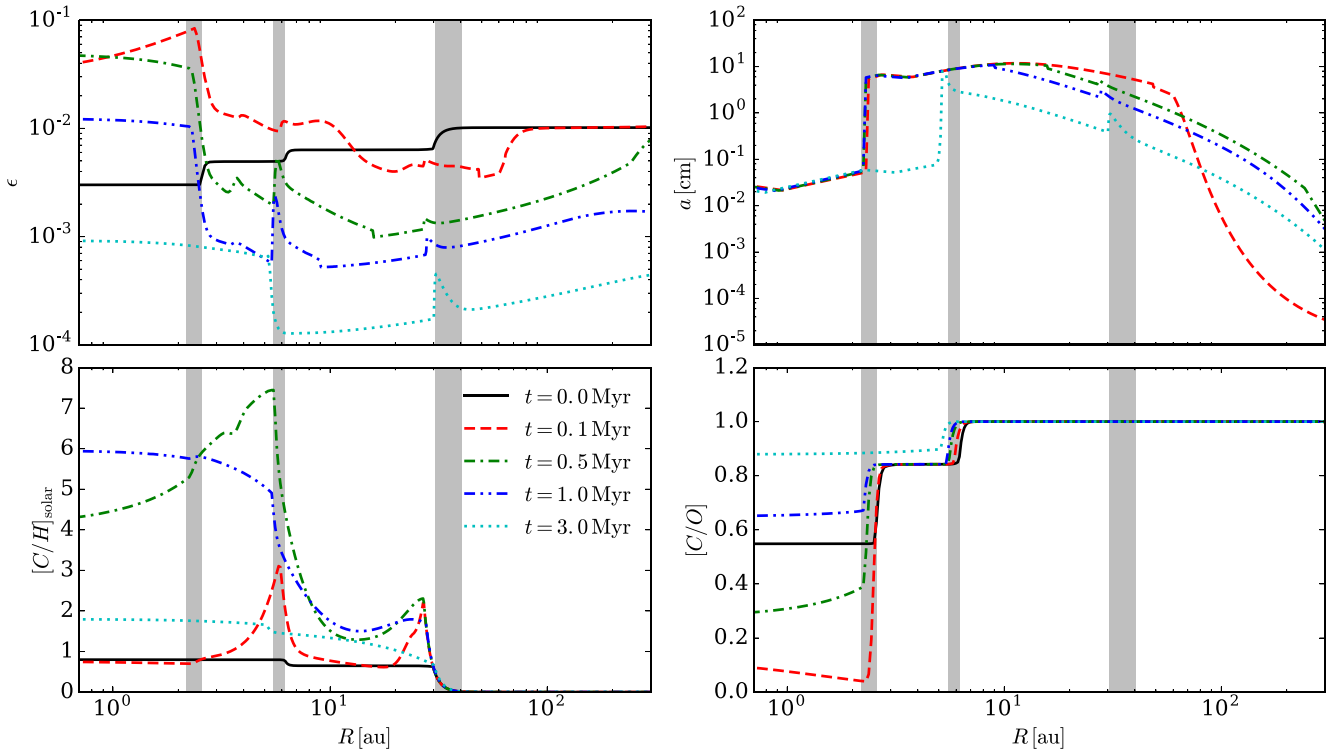

Figure 4. Same as Fig. 2, except for the Case 2 chemical equilibrium model.

CO abundance becomes high enough at the CO snow line that there is no longer enough oxygen available to maintain the equilibrium between CO and CO_2. From this point in time, the flux of CO_2 ice is controlled by the supply of oxygen (along with the original CO_2) to the CO snow line, which is continually decreasing (along with the dust-to-gas ratio). Thus, the CO_2 abundance between the CO and CO_2 snow lines decreases and the additional CO deposited between the snow lines begins to convert back to CO_2. Through this mechanism, the water abundance becomes depleted throughout the entire region between the CO and CO_2 snow lines. At this stage, the CO abundance between the snow lines may only continue to

change through advection and diffusion in the gas phase, similarly to the model in which reactions are neglected.

By increasing the CO_2 abundance on grains, this extra mechanism increases the flux of CO_2 to the CO_2 snow line, increasing the abundance of CO_2 there. Although some of the extra CO_2 is converted back to CO, no carbon-bearing species remain on the grains. Thus, inwards of the CO_2 snow line, carbon-bearing species are still only carried to the star by the gas phase advection and diffusion. The higher abundances of CO and CO_2 at the CO_2 snow line result in higher abundances of these species at all points interior to the CO_2 snow line.
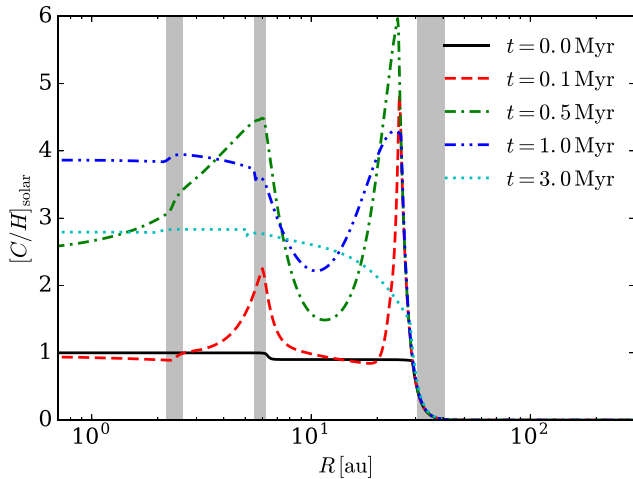
Figure 5. Evolution of the C/O and C/H ratios for the Case 1 chemistry. The evolution of the dust fraction and grain size is similar to the Case 2 chemical models, shown in Figs 2 and 4.

In addition to offering an additional way to transport CO inwards of the CO snow line, the imposition of equilibrium abundances allows a transport of CO_2 outwards from the CO_2 snow line. Normally, the diffusion of CO_2 outwards is prevented because any molecules that diffuse beyond their snow line condense on to the grains and are transported rapidly back to the snow line. However, in the equilibrium chemistry model, the extra CO at the CO_2 snow line is able to diffuse outwards without condensing out, which broadens the snow line outwards. The outward diffusion of CO can balanced by the conversion of CO into CO_2 and subsequently advection on the grains. However, the conversion of CO to CO_2 is again limited by the availability of oxygen, and thus the carbon enhancement at the CO_2 snow line can extend outwards to 10–15 au.

In the equilibrium models, the C/O ratio remains close to its initial value outside of the H_2O snow line as the fraction of CO and CO_2 molecules does not change. Inside of the water snow line, we see that C/O ratio evolves similarly in both models. This shows that despite the disc becoming depleted in water between the CO and CO_2 snow lines, radial drift is still delivering water to the inner disc. This occurs due to the conversion of CO_2 to CO at the CO_2 snow line, freeing up oxygen, which can then be transported inwards as ices.

For the Case 1 chemistry, the evolution is largely the same, shown in Fig. 5. The presence of CH_4 inside the CO_2 snow line means that the gas phase C/O ratio is higher than in the Case 1 chemistry, just as initial conditions. In both cases, the gas phase C/O ratio outside the water snow line is the same as the initial conditions, and thus the same as models in which the chemical composition is taken to be fixed (although the [C/H] ratio is not). The Case 1 chemistry produces a higher C/H ratio just inside the CO snow line than the Case 2 chemistry because a larger fraction of the carbon is in CO. Conversely, the C/H ratio is lower inside the CO_2 snow line because the CO_2 fraction is lower. The only significant difference between the two models is that inside the water snow line the C/O ratio remains sub-solar throughout the simulation because the conversion of CO into CH_4 at the CO_2 snow line continues to produce water ice long after the water that is initially delivered to the inner disc has been accreted.
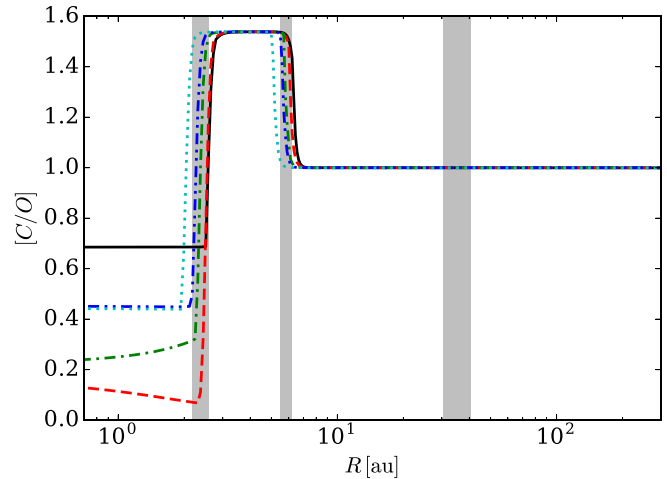
3.3 Viscosity dependence

Since the source and strength of turbulence responsible for accretion in protoplanetary discs is uncertain, we examine how these results are affected by changing the turbulent properties of the disc by varying α. In these models, we have chosen to keep the initial accretion rate fixed, adjusting the initial surface density along with α. We note that this choice makes little difference to the results because the radial drift velocity only depends on the Stokes number (equation 6) and the limiting Stokes number in both the radial drift-limited and turbulence-limited regimes (equations 12 and 13) also does not depend on the surface density normalization. However, the corresponding grain sizes are different. Thus, the main effects of varying α are, as α increases: (1) the time-scale on which the gas evolves viscously decreases, (2) the diffusion time-scale decreases and (3) the particle size decreases due to enhanced fragmentation.

We see from Fig. 6 that for $\alpha \lesssim 5 \times 10^{-3}$ the enhancement of the C/H ratio is similar in all models, with the main difference being that stronger diffusion at higher α broadens the spikes at the snow lines. We also see that by 3×10^6 yr the C/H ratio has dropped below the solar value for $\alpha = 5 \times 10^{-3}$. This is a consequence of the faster viscous evolution at higher α.

At $\alpha = 10^{-2}$, large C/H ratios are never reached. The faster diffusion and viscous evolution is one factor in determining this; however, this is compounded by the delivery of volatiles occurring more slowly than at lower α. The slower delivery of volatiles is due to grain growth in the $\alpha = 10^{-2}$ model being limited by high-velocity turbulent collisions rather than radial drift, resulting in a lower Stokes number (Fig. 7). For models with lower α, grain growth is limited by radial drift outside of 5–10 au instead. Since the radial drift limit does not depend on the level of turbulence or the surface density, in the drift-dominated regime the delivery of volatiles to the CO snow line is essentially identical. We note that the turbulent fragmentation also explains the disappearance of the spike in the [C/H] ratio at the CO_2 snow line for $\alpha = 5 \times 10^{-3}$: the maximum size of grains transitions from radial drift limited to turbulence limited between the CO_2 and CO snow lines in this model, reducing the flux of grains to the CO_2 snow line.
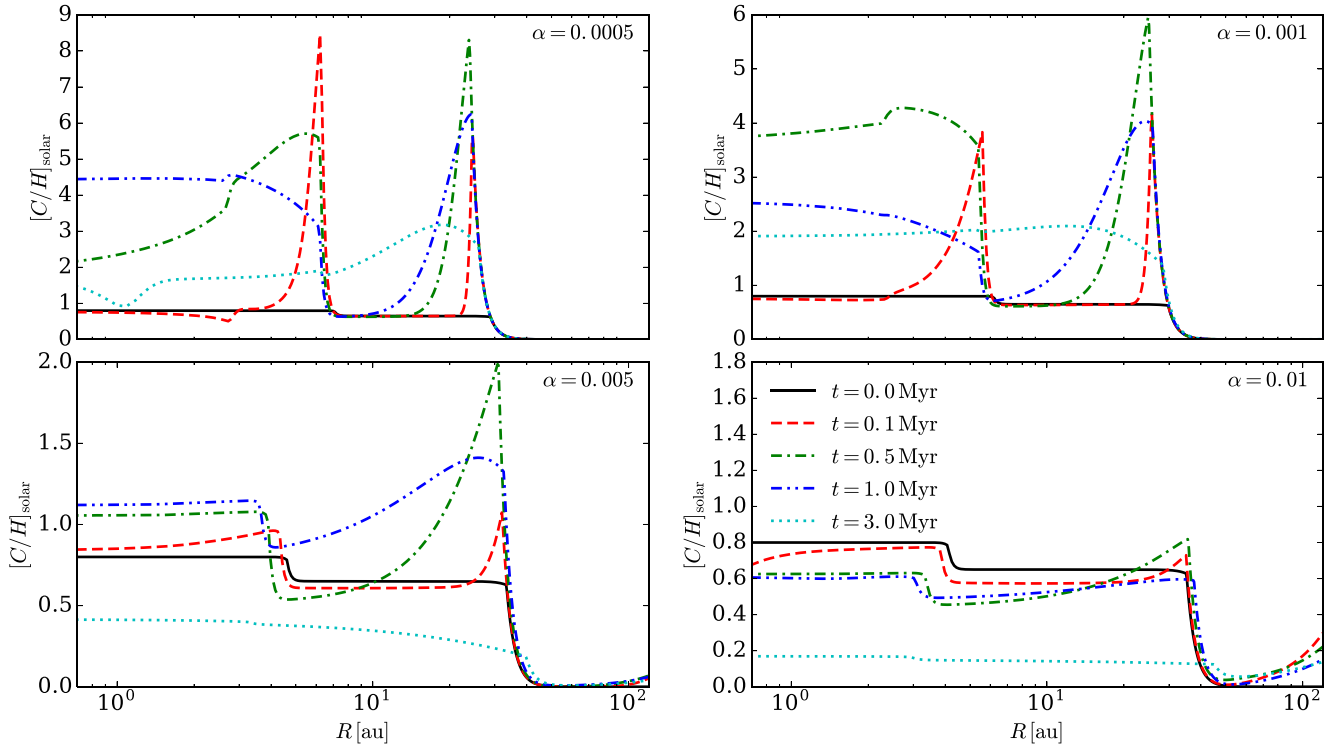
Figure 6. Evolution of the carbon abundance for different viscosity parameters, α. These models use the Case 2 chemistry ignoring chemical reactions.
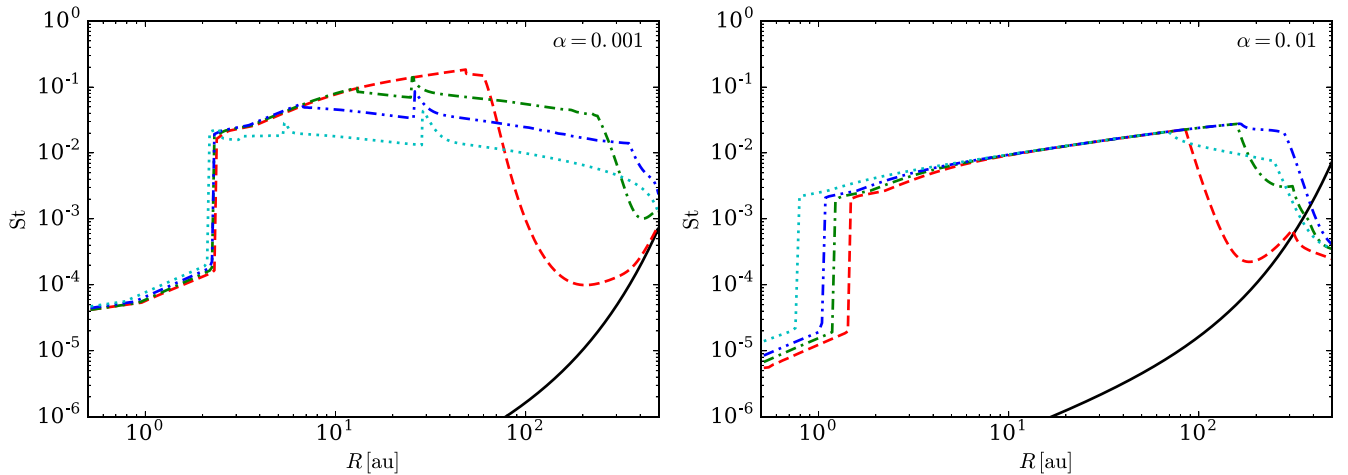

Figure 7. Evolution of the Stokes number for two different viscosity parameters, $\alpha = 0.001$ (left) and 0.01 (right). The line styles denote the same times as in Fig. 6. At $\alpha = 10^{-2}$, grain growth is almost entirely limited by turbulence. This results in a Stokes number that is independent of both the gas density and dust-to-gas ratio (equation 13). At lower viscosity, grain growth is instead limited by radial drift in the outer parts of the disc. Since the growth time is proportional to the dust-to-gas ratio, this results in lower Stokes numbers (equation 12). Within about 10 au, growth is limited by turbulence even at $\alpha = 10^{-3}$. The smaller Stokes numbers in the outer parts of the disc at early times are because the grains have not yet had time to grow to their maximum size.

These models also allow us to see how the results would change if the growth time-scale for dust was longer, e.g. due to bouncing preventing growth at large sizes. Slower growth means that radial drift will remove grains before they can become as large, thus reducing the Stokes number and also reducing the flux of ices into the inner disc. Diffusion and gas phase advection would thus be more effective at broadening the peaks near the snow lines. Therefore, a longer growth time-scale has a similar effect to increasing the turbulence. We note that the effect of slower growth will be less dramatic since increasing α affects both the radial drift and

diffusion, whilst slower growth only significantly affects the radial drift.

3.4 Disc size dependence

Fig. 8 shows how the size of the discs can affect the abundance evolution. In these models, the outer radius of the disc R_c has been varied, with all other parameters fixed. Since the disc mass is proportional to R_c, this means that the mass of the discs in these models varies. However, as noted above, the evolution is only very weakly
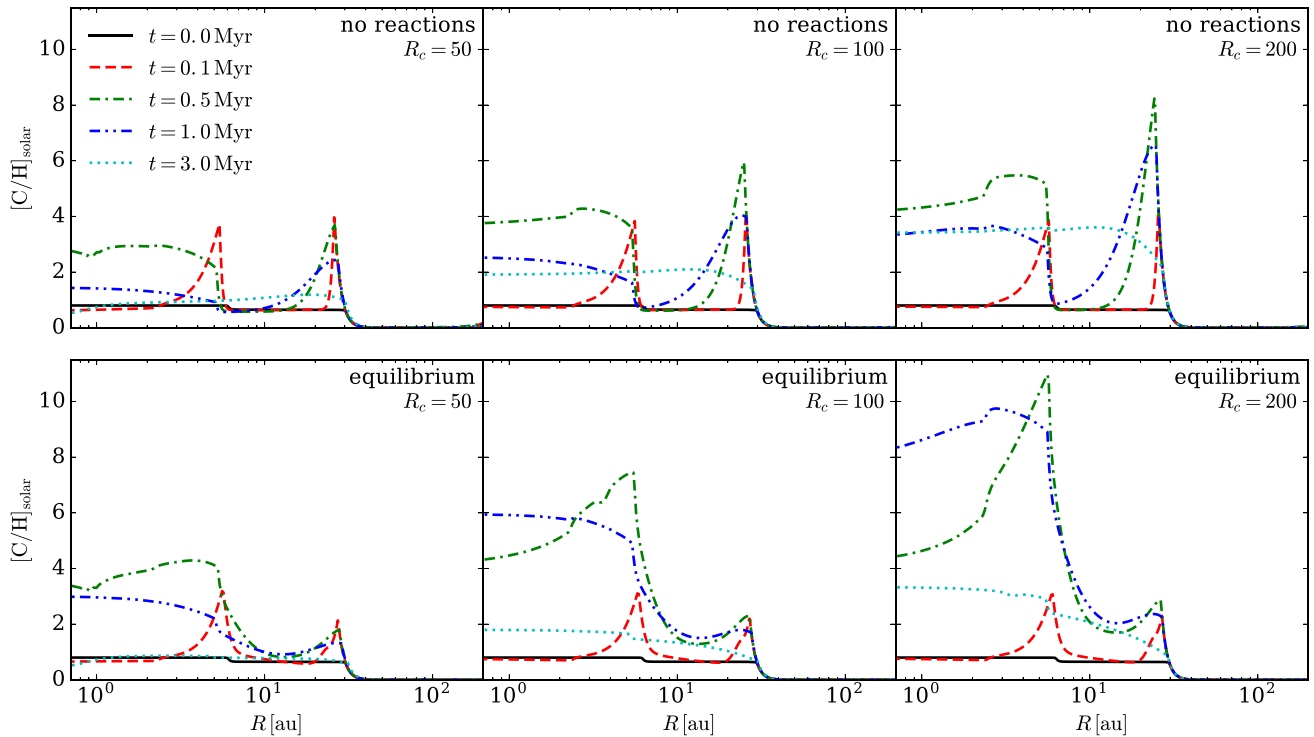
Figure 8. Evolution of the C/H ratio for Case 2 chemical models with varying outer radii, R_c. The top row shows models in which chemical reactions were neglected, while the bottom row shows models in which they were assumed to be fast enough that the equilibrium abundances were always maintained.

sensitive to the normalization of the surface density and thus the difference between these models is due to the different outer radii rather than different disc masses.

Considering first the model in which chemical reactions are assumed to be slow, we see that models with larger radii have the stronger C/H enhancements after 0.5 Myr, but prior to this time the abundance patterns are similar. This can be understood because growth time and radial drift time-scales are longer at larger and larger radii, so the pebble flux continues for longer in larger discs.

In the equilibrium chemistry model, the delivery of ices to the CO snow line behaves the same way; however, the conversion of CO to CO_2 prevents the build-up of a large C/H ratio at the CO snow line. Instead, the extra flux of CO and CO_2 ices is deposited at the CO_2 snow line, resulting in an even larger C/H ratio within 7 au.

4 PLANET ABUNDANCES

4.1 Formation and migration

The formation and evolution of planets via pebble accretion has been studied in detail in previous studies (e.g. Lambrechts et al. 2014; Bitsch et al. 2015), so we only discuss the essential features here. We shall focus on the formation of giant planets, which are relevant for Jupiter, Saturn and giant exoplanets. From Fig. 9, we see that giant planets tend to start their growth in the outer parts of the disc and migrate inwards. Within a critical radius (a few au to a few tens of au), the planets migrate too rapidly towards their star through Type I migration for them to accrete massive gaseous envelopes.

The precise details of evolution of the planet populations are model dependent. The most important parameters are the surface

density of the disc and the strength of the turbulent viscosity. Since the size of the disc affects how long the pebble flux continues, it can also affect how long giant planet formation occurs at a given location in the disc.[3] We explore planet formation in models with $R_c = 200$ for this reason, i.e. in order that giant planet formation may occur over a longer time. We investigate the model dependence using three models, two with initial accretion rates of 10^{-8} $M_\odot$ yr^{-1} but with different α (10^{-3} and 10^{-2}), and therefore different surface densities. In the final model, we use 10^{-9} $M_\odot$ yr^{-1} and $\alpha = 10^{-3}$, which gives the same surface density as the second model.

Fig. 10 shows considerable differences in the final location and masses of the planets formed in these models. First, we see that the second and third models, which have lower surface densities, can produce giant planets further in. Secondly, we see that increasing α at fixed surface density allows the planets to become more massive. Thirdly, in the outer disc, the growth of planets can be limited by the long growth time-scale associated with a low density of pebbles.

The innermost radius at which planets can accrete massive gaseous envelopes is controlled by the competition between growth and migration. When the pebble accretion rate is high enough, accretion during the envelope contraction phase dominates the time that the planet takes to grow before entering the runaway accretion phase. Since the accretion rate during envelope contraction does not depend on the surface density, but the migration rate is proportional to the surface density, this means that planets reach runaway

---

[3] In the inner disc, the temperature structure can also be important for controlling the location of planet traps. Since the cores of giant planets tend to form further out, the locations of these planet traps are less relevant for our study.
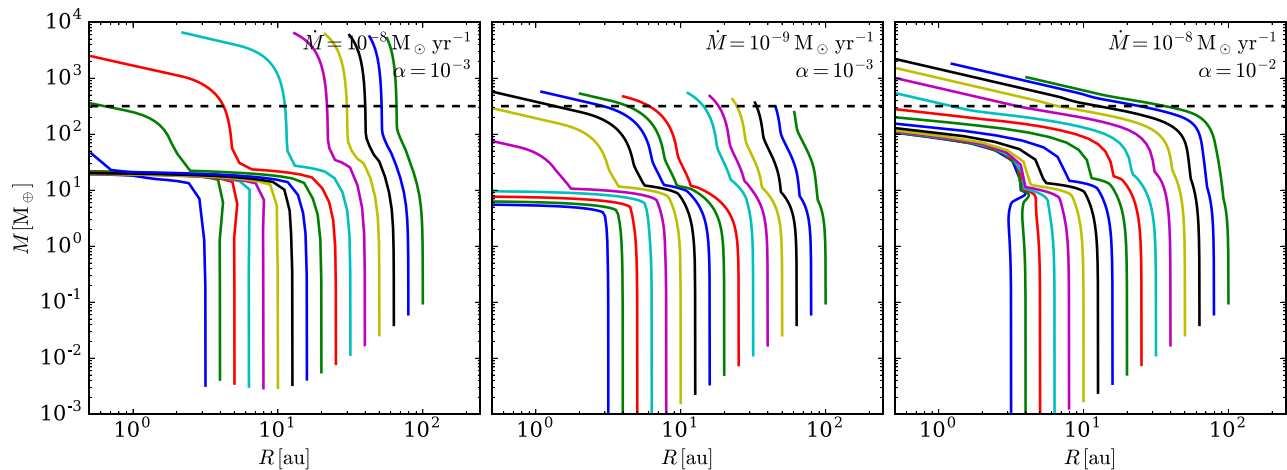
Figure 9. Evolution of planet masses and radii up to 3 Myr for different disc models. Each line shows a single track for a planet as it grows and migrates. The tracks shown are for planets forming at the start of the simulation, but planets that form later undergo similar evolution but only reach lower masses by 3 Myr. The dashed black lines show the mass of Jupiter.
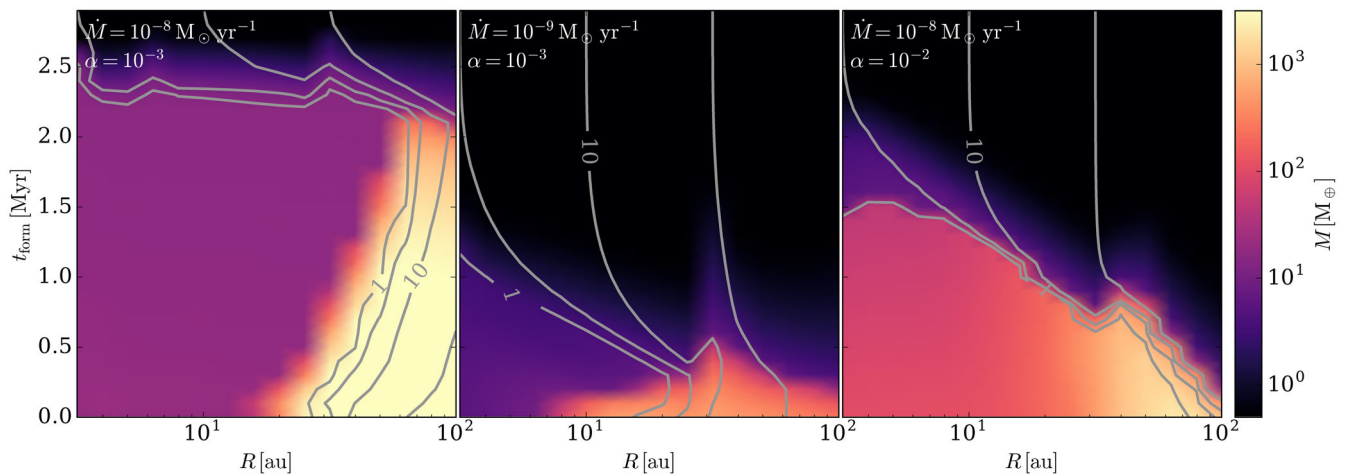

Figure 10. Final masses and locations of planets formed in models with different accretion rates and turbulent viscosities. The x- and y-axes show the initial formation time and location of the planetary embryo. The colour shows the final planet mass at 3 Myr and the contours show the final location, in au.

accretion after less migration at larger distances, or in lower mass discs. In the two models with $\alpha = 10^{-3}$, this explains why the model with the lower accretion rate (and therefore surface density) is able to form giant planets at smaller radii (at $t = 0$ Myr): they have a longer time in which to grow via envelope contraction. However, once the discs have evolved, the surface density of pebbles in the lower mass disc becomes too low and the planetary embryos do not accrete gaseous envelopes within 3 Myr.

In addition to the competition between envelope contraction and migration, a second effect is important for determining the outcome of planet formation. This effect is illustrated by comparing the two models with the same initial surface density, but different α and $\dot{M}$. Here we see that increasing α leads to more massive planets, despite stronger turbulence limiting the particle size. The smaller particle size means that the pebble accretion rate at a given surface density is lower, but the radial drift of particles is also slower. Thus, in the outer disc, the cores become more massive before the surface density of pebbles drops. The larger core mass allows for faster gas accretion during the envelope contraction phase resulting in larger planet masses.

If we focus on the origin of giant planets, we see that they form from embryos that typically originate from far outside the water snow line. Neptune- to Saturn-mass planets may form further in, depending on model parameters. However, we note that when it comes to assessing the chemical abundance patterns of giant planets formed by pebble accretion, the differences between the models make only a moderate difference. As Fig. 9 shows, we find that giant planets may accrete their envelopes at a range of locations within the disc. In high-density environments, migration can prevent planets from accreting their envelopes within water snow line (~3 au). However, we see that planets that end as hot Jupiters can accrete a significant amount of their mass inside the water snow line. In our models, the giant planets always continue to accrete gas as they migrate; however, this may not be the case in reality. This caveat, along with the possibility of continued migration after the disc has dispersed (through dynamical interactions or the Kozai–Lidov mechanism; Kozai 1962; Lidov 1962), means that it may be possible to form hot Jupiters that have accreted their envelopes outside of the water snow line. The converse is not true however: i.e. planets that end up outside the water snow line are
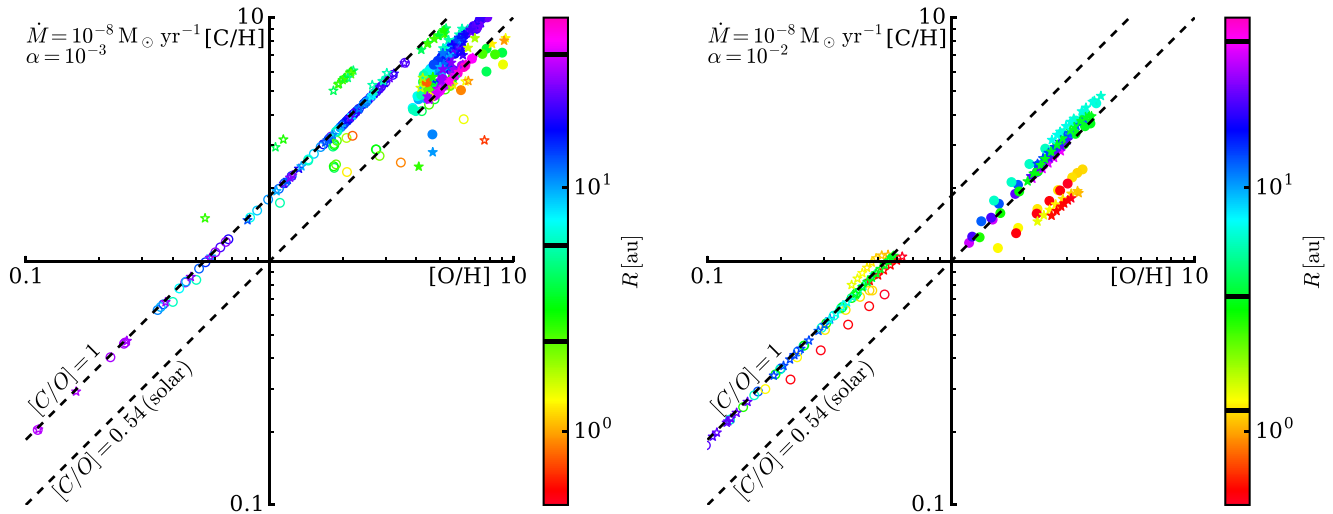
Figure 11. Carbon and oxygen abundances of planets at 1 M_J, formed in a disc with $R_c = 200$ and an initial $\dot{M} = 10^{-8}$ $M_\odot$ yr^{-1}. Left: the standard model with $\alpha = 10^{-3}$. Right: high-viscosity model with $\alpha = 10^{-2}$. The abundances are given relative to the solar abundances. Stars correspond to the Case 1 equilibrium abundance chemical model, while circles correspond to the Case 2 non-equilibrium abundances. Open symbols denote the abundance of the gaseous envelope, while filled symbols denote the total abundance of both the envelope and core. The colour denotes the location of the planets when they reach 1 M_J and the horizontal black lines on the colour bar denote the locations of the water, CO_2 and CO snow line (from inside to out). See Section 4.2 for an explanation.

unlikely to have accreted their envelopes within the water snow line because disc-driven migration is always inwards (unless planet–planet scattering occurred; e.g. Lega, Morbidelli & Nesvorný 2013).

4.2 Chemical abundances

We now consider the chemical abundance patterns of giant planets that form in our chemically evolving disc models. While the details of the planet formation process such as the final mass and location of the planets are dependent on the planet formation prescription, the chemistry of the planets formed is much less so. Therefore, we focus on the abundances of planets forming in the standard model with $R_c = 200$ au, $\dot{M} = 10^{-8}$ $M_\odot$ yr^{-1} and $\alpha = 10^{-3}$. The one exception to this case is when grain growth is suppressed, for example due to strong turbulence driving fragmentation. In this case, the radial drift occurs more slowly resulting in a smaller enrichment of the disc. Taking this to the extreme, when radial drift becomes negligible, the chemical abundances remain close to their initial values.

The C/H and O/H ratios together provide a useful way of determining how and where the planet formed. They key to this is that inside the CO snow line, the grains always have a C/O ratio that is sub-solar (C/O = 0.54). Conversely, the gas has C/O ratios that are above 0.5, except inside the water snow line. Thus, C/O ratios above solar can be used to infer that carbon was predominantly accreted as gas, rather than solids. In this section, we demonstrate how the C/O ratio combined with the C/H ratio can be used to infer the location in which the planet formed. To this end, we place the planets formed in our models on this diagram in Fig. 11, when the planets reach the mass of Jupiter.

When the gas is not significantly enriched by radial drift, we find that only one of the C/H and C/O ratios may be significantly super-solar. Similar abundance patterns were found in previous models that neglected radial drift (e.g. Madhusudhan et al. 2014a, 2016). One such case is the model with $\alpha = 10^{-2}$, as shown in Fig. 11. Here the accretion of gas alone produces planets with C/H ratios that are sub-solar, but C/O ratios between solar and C/O = 1, independently of where they form. Therefore, in order to produce super-solar C/H

ratios, some enrichment by solids is needed, either through erosion of the core or enrichment by planetesimals. Typically, this produces a sub-solar C/O ratio because the ices are oxygen rich. Only outside the CO snow line does the C/O ratio in the ices become solar. Pebble accretion in such environments can produce a *slightly* super-solar C/O ratio because the cores of giant planets may migrate a long way before accreting their gas (see Fig. 9). Thus, planets can form cores outside the CO snow line, which have solar C/O ratios and then accrete their gas inside the CO snow line, where the gas has C/O = 1. However, while this may produce C/O ratios above solar, this will never produce a C/O ratio close to unity, unless the C/H ratio remains sub-solar.

Conversely, the envelopes of giant planets may have C/H and C/O ratios that are both super-solar if they accrete metal-rich gas. This is made possible by the radial drift of large grains, which carry volatile species to their ice lines, enriching the gas when they sublimate. These volatiles may then spread inwards, enriching the entire region inside of their snow lines. In what follows, we first consider the compositions of gaseous envelopes formed by accreting metal-rich gas, *without* any enrichment by solids. Subsequently, we discuss the effects of enrichment.

The C/O ratio of planets that accrete their envelope outside the CO_2 snow line is always 1 (neglecting enrichment by solids). This is because CO is the only carbon- or oxygen-bearing species in the gas phase. However, due to radial drift, the C/H ratio of planets with C/O = 1 varies considerably due to the large variation in the C/H of the disc, both radially and temporally. Between the CO and CO_2 snow line, the C/H ratio of the disc is super-solar, and thus planets that accrete their envelopes here also have super-solar C/H ratios. Outside the CO snow line, the gas phase C/H ratio is negligibly small, so planets that accrete their entire envelopes outside the CO snow line would be off the bottom left of Fig. 11. Those planets that do have C/O = 1 and C/H of solar or slightly below can be formed in two ways. Either they accreted part of their envelopes in the CO depleted gas from outside the snow line along with some CO-rich gas inside the snow line or they accreted their envelopes late in the disc's evolution once the global C/H ratio has dropped.

Planets that accrete their envelopes inside the CO_2 snow line have C/O $\neq$ 1 because CO_2 and CH_4 also contribute to the carbon and oxygen abundance. The C/O ratio differs between the models due to the different amounts of these species present, but all models predict C/O $\neq$ 1. If chemical reactions occur more slowly than radial drift, the gas between the CO_2 and H_2O snow lines is dominated by CO_2 so we find C/O $\approx$ 0.5–0.6, i.e. close to solar. If instead chemical reactions are fast enough to maintain chemical equilibrium between the carbon- and oxygen-bearing species, the C/O ratio remains close to its initial value in this region, i.e. C/O $\approx$ 1.5 and 0.85 for the Case 1 and 2 models, respectively. The C/H ratio can vary considerably depending on the exact location and model, but the C/H ratio between the CO_2 and H_2O snow lines is generally super-solar when radial drift is efficient.

Sub-solar C/O ratios are only produced by gas accretion when planets accrete their envelopes inside the H_2O snow line. Even in this region we typically find that radial drift produces C/H ratios that are super-solar and thus there is a region of the C/H and O/H parameter space that does not contain any planets (where the O/H ratio above solar and the C/H ratio is less than about twice solar). The precise size of this region is again likely to be model dependent, but similarly to models that neglect radial drift, planets do not form with super-solar O/H and sub-solar C/H. Fig. 11 contains relatively few planets in this region because many of the planets that accrete a significant fraction of their envelope inside the H_2O snow line end up with masses of several Jupiter masses. For this reason, hot Jupiters that have a super-solar C/H ratio and a sub-solar C/O ratio may be more frequent than the density of points in Fig. 11 suggests.

The accretion of chemically enriched gas leaves clear signatures in the abundances of giant planets. This can be recognized through planets that have C/O and C/H ratios that are both higher than that of their host star, since these abundances cannot be reached when enriching the atmosphere with solids. Furthermore, because the gas is dominated by CO beyond the CO_2 snow line, accurate measurements of the C/O ratio will be able to determine whether the planet formed outside the CO_2 snow line or not.

In the case of metal enrichment via solids, it may be possible to determine whether these solids were accreted through planetesimals or partially dissolving the core. This is possible because C/O ratios above solar only appear if the solids were accreted outside the CO snow line, but the gas was accreted inside it. Since enrichment via planetesimal accretion cannot happen before the envelope is accreted, this cannot occur without invoking outward migration. Finally, the combined gas of both metal-enriched gas accretion and subsequent enrichment by solids should be identifiable through a population of planets with very high C/H ratios ($\gtrsim$5) and C/O ratios between roughly solar and C/O = 1.

4.3 Jupiter and Saturn

In comparison to exoplanets, the chemical abundances of the Solar system giants are uniquely well determined. Jupiter is known to be metal rich, with a C/H ratio that is three to five times solar (Owen et al. 1999), along with super-solar abundances of nitrogen, sulphur and noble gases. However, the water abundance is still uncertain. Observations of a hotspot made by the Galileo probe suggest a vastly sub-solar O/H ratio, but this may not be representative of Jupiter's bulk abundance. On the other hand, thermochemical modelling of Jupiter's structure suggests that the water abundance should not be enhanced more than about eight times solar (Visscher et al. 2010), and thus the C/O ratio should not be lower than about half of the solar value. For Saturn, the abundance pattern appears similar, but with a

C/H ratio of about eight times solar (Atreya et al. 2016). Although the C/O ratio of the Solar system giants is currently unknown, *Juno* will soon measure Jupiter's water abundance (Matousek 2007), which can be used to constrain models of planet formation.

Planet formation models constrain Jupiter and Saturn to be somewhere close to its current location during the terrestrial planet formation era (Raymond et al. 2014, and references therein), ruling out disc-free migration modes for them. Therefore, we know that they likely accreted their envelopes somewhere near their current locations, unless gas accretion can be stopped without stifling migration.

At ∼5 au, Jupiter likely accreted its gaseous envelope somewhere close to or inside the CO_2 snow line, which is at 7 au in our models. For models that produce a Jupiter-mass planet close to its current location, we find that the equilibrium chemistry for both Cases 1 and 2 are easily able to produce C/H ratios in the envelope that are four to five times solar. However, if the reactions are slow, then the delivery of CO molecules to the CO_2 snow line is slower and the C/H ratio is instead 2.5–3.5 times solar, compatible with estimates at the lower end of the range for Jupiter.

The C/O ratio of our Jupiter models depends on which side of the CO_2 snow line Jupiter accreted its mass. If Jupiter accreted its envelope outside the CO_2 snow line, then it should have C/O $\approx$ 1. While different chemical models make differing predictions for the C/O ratio if Jupiter accreted its envelope inside the CO_2 snow line, in general we find that the C/O ratio differs from C/O $\approx$ 1. The Case 2 no reaction model produces C/O $\approx$ 0.5 because the carbon abundance is dominated by CO_2 inside the CO_2 snow line in this case. For the equilibrium models, the C/O ratio remains close to the initial values (Fig. 1), producing a C/O ratio of 1.5 and 0.8 for Cases 1 and 2, respectively. We also find models that accrete similar amounts of mass on both sides of the snow lines, in which case the C/O ratio can be intermediate between these values.

Forming Saturn without solid accretion is more problematic because its C/H ratio is observed to be eight times solar. At 9.5 au, its Saturn is outside of the CO_2 snow line, but also a long way from the CO snow line. Even in the most optimistic of our models, Saturn would need to have accreted its envelope very close to the CO snow line to produce a sufficiently high C/H ratio. For this reason, the enrichment of Saturn's atmosphere by solids is appealing. From such models, we expect [C/O] $\approx$ 0.6–0.7.

We note that it might be surprising to find that the metals in Jupiter's atmosphere were accreted as metal-rich gases, but in Saturn they arrived in solids. Thus, one might expect *Juno* to find that Jupiter has a significantly sub-solar C/O ratio. A second possibility would be that Saturn accreted its envelope inwards of its current location, close to the CO_2 snow line, and migrated outwards to its current location. Such outward migration is proposed by the grand-tack model of terrestrial planet formation (Walsh et al. 2011). However, some enrichment by solids is likely required, otherwise highly favourable conditions for gas enrichment such as low turbulence ($\alpha < 10^{-3}$) in the inner disc or a large outer radius ($\gtrsim$200 au) would still be needed in order to produce high enough C/H ratios.

5 DISCUSSION

5.1 Disc evolution

In this work, we have investigated the redistribution of the dominant carbon- and oxygen-bearing species in evolving protoplanetary discs, along with the associated impact on the chemical abundances of giant planets that form in such discs. The radial drift of icy grains

from the outer disc can supply volatiles to the inner disc on shorter time-scales than they can be carried away by gas phase diffusion or advection, resulting in the enhancement of volatiles at the snow lines. As the disc evolves, these enhancements spread inwards, enriching the gas phase C/H ratio in the inner disc by factors of a few to several.

A side effect is the segregation of molecular species in the disc. CO molecules are predominantly left at 20–30 au, near the CO snow line, while CO_2 and water travel further in before being left behind at their own snow lines. Inside the CO and CO_2 snow lines, this drives the C/O ratio towards that of the dominant species. However, chemical reactions will play an important role in determining how strong the change in C/O ratio is because they may be able to remove some of the excess molecules. We explored the effect chemical reactions have on radial transport by considering two limiting cases: (1) the case where they occur on time-scales longer than the time-scale for disc evolution, which we model by neglecting them entirely; (2) the case where the chemical time-scale is fastest time-scale, modelled by resetting the molecular ratios to their initial ('equilibrium') values. In the first model, the C/O ratio inside each of the snow lines becomes dominated by their respective molecules (e.g. CO inside the CO snow line), while in the second the C/O ratio stays close to the initial value. In practice, the time-scale for chemical reactions lies between these extremes (Eistrup et al. 2016 estimate a few 10^5 yr) and thus the degree to which the local abundances are dominated by the species deposited at each snow line will also fall between the two extremes.

In addition to restoring the initial C/O ratio, rapid chemical reactions also enhance the transport of carbon inside the CO snow line, resulting in a greater fraction of the carbon-bearing species being deposited at the CO_2 snow line. This also introduces differences into the late phase of the disc's evolution, once the flux of ices has fallen, which is governed by viscous accretion. During this phase, the chemical abundances are dominated by the gaseous species, so the evolution can be understood by considering only the gas. Since accretion removes mass sequentially from inside to out, the water-rich inner disc is cleared first and is replaced by the carbon-rich gas that has moved in from between the water and CO_2 snow lines; thus, the C/O ratio becomes constant throughout the region inside of the CO_2 snow line. Accretion then removes the gas that was initially inside the CO_2 snow line and the C/O ratio tends to unity as the whole disc becomes dominated by the CO-rich gas from outside of the CO_2 snow line. Since a greater proportion of the carbon-bearing molecules are deposited at the CO_2 snow line in the case of rapid chemical reactions, the C/H ratio also decreases faster because it is accreted earlier.

At the snow lines, we find an enhancement in the dust-to-gas ratio of up to factors of a few. The peak of the solid density occurs just outside of the peak of the vapour concentration. This peak is driven by the outward diffusion and recondensation of ices on to grains that are just outside the snow line. Unsurprisingly, these results agree with Schoonenberg & Ormel (2017), who model essentially the same processes: radial drift, diffusion and thermal adsorption and desorption. We also see that where the grains transition from being icy to ice-free, there is a jump in the surface density, which occurs inside the snow line. In our model, this arises because the ice-free grains fragment more easily, as was reported by Cridland, Pudritz & Birnstiel (2017) who used a similar model for the water snow line. Schoonenberg & Ormel (2017) also find similar behaviour if the grains have the structure of many small silicate cores held together by ices. In this case, sublimation drives fragmentation. Sintering also gives rise to a similar effect (Saito & Sirono 2011).

Stammler et al. (2017) have conducted a similar study into the structure of the CO snow line. They neglected fragmentation and instead find a different behaviour, that the growth of grains driven by the extra adsorption of ices outside the snow line leads to larger grains that drift faster. Neglecting fragmentation at the CO snow line is likely a valid assumption, because the collision velocities are lower and the water ices remain on the grains and so collisional fragmentation is not expected. However, at the water snow line, there is likely to be a complex interplay between growth and fragmentation. Whether an enhancement in the dust-to-gas ratio should be expected at the water snow line will depend on the details of grain growth and fragmentation. However, these differences are unlikely to have much of an effect on the evolution of the chemical abundances, because the mass trapped outside the snow line is a relatively small fraction of the volatile abundance inside the snow line.

Our suggestion that radial drift should lead to chemical enrichment in the inner disc is in tension with observational constraints. For example, thermochemical modelling of HD, CO and carbon lines in TW Hydrae suggests that carbon should be depleted by perhaps as much as a factor of 100, along with a C/O ratio that might be above unity (Favre et al. 2013; Du, Bergin & Hogerheijde 2015; Bergin et al. 2016; Kama et al. 2016; Manara et al. 2016). These observations are somewhat difficult to reconcile with our models, which suggest that CO should be enhanced by radial drift. One possibility is that a greater fraction of the carbon-bearing species is locked up in ices than is predicted by models. This might change the detailed abundances of our models by altering the transport of the volatiles, but the phenomenology should not be affected. Alternatively, the low C/H ratio can be achieved during the vary late phase of our models, once the majority of the CO and CO_2 has been accreted on to the star. In this case, the low C/H ratio should be associated with a low dust-to-gas ratio. In many of our models, the dust-to-gas ratio drops to a few 10^4 before the CO in the inner disc is accreted because the dust evolution is much faster than the gas evolution. Therefore, in order to achieve low C/H before exhausting the disc of dust, it may be necessary to invoke high viscous α. This both accelerates the accretion of CO and limits dust depletion: high α promotes dust fragmentation and hence, by limiting particle size, slows down radial drift. Given that TW Hydrae may have a relatively high accretion rate, this may be a reasonable explanation (Brickhouse et al. 2012).

Another suggested explanation for the depleted C/H is that most of the carbon is in the form of refractory organic molecules. If this explanation is true, then the enhancement of the C/H at the snow lines would not occur as the refractory carbon would remain on the grains. However, there is good observational evidence that refractory species cannot dominate the carbon abundance. In Herbig Ae stars, the long mixing time-scale means that the abundance of the stellar atmosphere can be used to measure the abundance of the gas accreted. Kama, Folsom & Pinilla (2015) showed that in transition discs with large holes the gas accreted is depleted in refractory elements such as Fe, Mg and Si, while non-transition discs showed no depletion. This can be taken as evidence that the transition objects were accreting gas that is depleted of dust, as would be expected if planets are responsible for opening up gaps in the disc. However, both transition and non-transition discs have stellar carbon and oxygen abundances that are compatible with solar values, which is strong evidence that neither of these species can be predominantly in refractory species on the grains. One possible solution to this problem is conversion of CO into CO_2 ice (e.g. Eistrup et al. 2016), in which case we would

expect the chemical enrichment to follow our equilibrium abundance models.

There is also evidence that disc evolution can proceed as we model it here, i.e. with the radial drift of grains occurring on time-scales shorter than the gas evolves. The numerous discs in which the dust radii are observed to be smaller than their gas radii (Guilloteau et al. 2011; Andrews et al. 2012; Birnstiel & Andrews 2014; Piétu et al. 2014) provide evidence for ongoing radial drift. Furthermore, there are now a number of debris discs known that have low dust masses (such as HD 141569 and HD 21997), but still have large amounts of gas as traced by ^{18}CO and ^{13}CO (Matrà et al. 2015; Wyatt et al. 2015; Pericaud et al. 2017). The CO masses derived are too high to be compatible with a cometary origin for CO, suggesting that it must be primordial (Kóspál et al. 2013; Thi et al. 2014). These objects provide an ideal laboratory to test our models against disc evolution. We should expect to see a high C/H ratio due to the radial flux of ices, and an inner disc that is depleted in water since it will likely have been accreted on to the star. These objects should also have super-solar C/O ratios.

5.2 Planet formation

We have examined the carbon and oxygen abundances of planets that form in evolving discs. While there are considerable differences between the evolution tracks of planets forming at the same location in different disc models, the chemical abundances of the planets only depend on where they accreted their envelopes. A key feature of the radial drift of ices is that the gas phase abundances of the dominant carbon and oxygen carriers can become enriched. This means that giant planets with metal-rich atmospheres need not have enriched their atmospheres by the accretion of solids (through either planetesimal accretion or a partially dissolved core).

The formation of metal-rich atmospheres by the accretion of metal-rich gas produces clear signatures in the C/O ratio, which can be used to determine that their abundances came from gas accretion rather than solid accretion. Furthermore, the C/H and C/O ratios can be used to determine *where* in the disc the planets formed in relation to the various snow lines. The explanation for this difference comes from the fact that inside the CO snow line the composition of ices is always oxygen rich (C/O less than solar), while with the exception of inside the H_2O snow line the C/O ratio is always close to solar (CO_2-dominated gas, C/O = 0.5) or super-solar.

Since these high C/O and C/H ratios cannot be formed by enrichment of the atmospheres by solids, the discovery of planets with such abundances can be used to constrain the evolution of the discs in which they formed. The formation of planets with a low C/O and high C/H ratio remains possible through enrichment by solids, or accretion of the envelope within the water snow line. According to our models, planets with low C/H ratios must have formed beyond the CO snow line, or late in the disc's evolution once the pebble flux has dropped and the C/H ratio has decreased through accretion on to the star.

By putting upper limits on the amount of solids accreted by giant planets, it may be possible to constrain planet formation models. For example, in the case of a planet with a precisely determined C/O ratio that is close to unity, along with a high C/H ratio, we can be sure that it accreted its metals through the accretion of metal-rich gas from outside the CO_2 snow line. It may thus be possible to put an upper limit on the amount of solids accreted and thus limit the surface density of planetesimals in the disc. Given the need for high planetesimal surface densities for planetesimal

accretion to be efficient (Kobayashi et al. 2011), along with the fact that a high gas phase C/H ratio implies significant radial drift and the presence of pebbles, the existence of such planets may be able to distinguish giant planet formation by pebble accretion from planetesimal accretion.

Current observations of hot Jupiters are often consistent with either elevated C/O ratios or possibly C/O ratios close to that of their host star as the uncertainties remain significant (e.g. Line et al. 2014; Madhusudhan et al. 2014a; Kreidberg et al. 2015; Brewer et al. 2017). Estimates of the O/H (and thus C/H) ratios for these planets inferred from H_2O abundances have produced a wide range of abundances that vary from consistent with solar to highly subsolar. All current planet formation models require formation outside of the CO snow line to produce such low O/H or C/H ratios, so it is already clear that some planets may have formed far out in the disc. For those with an O/H ratio closer to solar, more accurate C/O and C/H ratios should be able to determine how they accreted their metals.

For the Solar system giants, the uncertainty in their C/O ratio means that we cannot yet be sure how or where they formed. However, *Juno* will soon make this measurement (Matousek 2007). Our models make clear predictions for Jupiter's C/O ratio based on its formation location. If Jupiter accreted its metals through the accretion of metal-rich gas, then we expect C/O ≥ 0.5, i.e. close to solar and above, rather than sub-solar as would be expected for the accretion of solids. If *Juno* finds that Jupiter has C/O = 1, then we expect Jupiter to have formed outside the CO_2 snow line, while C/O > 1 would imply that Jupiter formed in a methane-rich environment inside the CO_2 snow line, while 0.5 < C/O < 1 also implies formation inside the CO_2 snow line, but in a CO_2-rich environment.

6 CONCLUSIONS

We have investigated the enrichment of the gas phase metallicity in discs and giant planets that is associated with the radial drift of icy grains from the outer parts of the disc. By following the condensation and evaporation of the dominant carbon- and oxygen-bearing species, CO, CO_2, CH_4 and H_2O, we are able to determine how the C/H, O/H and C/O ratios evolve as the disc evolves. Since the radial drift of dust grains is typically faster than the gas evolution, this leads to enhancements in the metallicity of the disc near the snow lines, where the molecules sublimate. Near the snow lines, this can result in enhancements of up to a factor of 10 in the C/H or O/H ratios. These enhancements can then spread inwards as the gas phase molecules diffuse and are carried towards the star along with the gas, enriching the entire disc inside the CO snow line (located at about 30–40 au). The enhancement of the C/H and O/H ratios in the disc opens up the possibility that giant planets may become metal rich by accreting metal-rich gas directly, rather than requiring subsequent enhancement by the accretion of solids (either through the accretion of planetesimals or dissolving part of the planet's core into the envelope).

The accretion of metal-rich gas can produce planets with C/H and C/O ratios that are both super-solar. This region of parameter space cannot be reached by enrichment of the atmosphere due to solids alone, because the C/O ratio of icy dust grains is always sub-solar (Öberg et al. 2011). Thus, the detection of planets with C/O and C/H ratios that are both super-solar is clear evidence that the majority of the planet's metals were accreted from metal-rich gas. By determining limits on the amount of solids accreted in the form of planetesimals, it may be possible to put upper limits on the surface density of planetesimals present in the disc when the planet

accreted its envelope. Given the need for a relatively high surface density of planetesimals for traditional core accretion models to form giant planets (Pollack et al. 1996; Kobayashi et al. 2011), it may thus be possible to determine whether such a planet formed by planetesimal accretion or pebble accretion.

Furthermore, the C/O ratio and C/H ratio of the planet can be used to constrain where the planet accreted its envelope. For example, outside the CO_2 snow line, the gas phase carbon abundance is dominated by CO and thus the C/O ratio is close to 1. Similarly, we find that C/O ratios below about solar are only possible if the planet accreted its envelope inside the H_2O snow line, and thus very oxygen rich hot Jupiters would favour *in situ* formation scenarios. Additionally, the C/H ratio can be used to infer where the planet formed in relation to the CO snow line, since outside of the CO snow line all of the dominant carbon-bearing species are frozen out on to grains, and thus the planets should have C/H ratios that are much smaller than solar.

A similar argument can be applied to Jupiter to determine where it formed. Although Jupiter's C/O is currently poorly known, the *Juno* satellite will soon provide a measurement (Matousek 2007). Given that Jupiter's current location (∼5 au) is close to the CO_2 snow line (located at 7 au in our models), depending on how far it migrated Jupiter may have accreted its envelope on either side of snow line. If *Juno* measures a C/O ratio close to unity, this would be good evidence that Jupiter formed outside of the CO_2. Our predictions for Jupiter's abundance if it formed inside the CO_2 snow line are dependent on assumptions made in the chemical evolution model, but we expect C/O $\neq$ 1. Since none of our models produce C/O ratios that are below solar, a sub-solar C/O ratio measurement would support the idea that Jupiter's metals were instead delivered by the accretion of solids.

7 MATERIALS

In the interest of reproducibility, the code used to generate the models in this paper has been made freely available and can be found on github.

REFERENCES

Agnor C. B., Lin D. N. C., 2012, ApJ, 745, 143
Ali-Dib M., 2017, MNRAS, 464, 4282
Alibert Y., Mordasini C., Benz W., Winisdoerffer C., 2005, A&A, 434, 343
Andrews S. M. et al., 2012, ApJ, 744, 162
Asplund M., Grevesse N., Sauval A. J., Scott P., 2009, ARA&A, 47, 481
Atreya S. K., Wong A.-S., 2005, Space Sci. Rev., 116, 121
Atreya S. K., Crida A., Guillot T., Lunine J. I., Madhusudhan N., Mousis O., 2016, in Baines K. H., Flasar F. M., Krupp N., Stallard T. S., eds, The Origin and Evolution of Saturn, with Exoplanet Perspective, Saturn in the 21st Century, 2015. Cambridge Univ. Press, Cambridge
Bai X.-N., Stone J. M., 2010, ApJ, 722, 1437
Baruteau C. et al., 2014, Protostars and Planets VI. Univ. Arizona Press, Tucson, p. 667
Bath G. T., Pringle J. E., 1981, MNRAS, 194, 967
Bell K. R., Lin D. N. C., 1994, ApJ, 427, 987

Bergin E. A., Du F., Cleeves L. I., Blake G. A., Schwarz K., Visser R., Zhang K., 2016, ApJ, 831, 101
Birnstiel T., Andrews S. M., 2014, ApJ, 780, 153
Birnstiel T., Dullemond C. P., Brauer F., 2010, A&A, 513, A79
Birnstiel T., Ormel C. W., Dullemond C. P., 2011, A&A, 525, A11
Birnstiel T., Klahr H., Ercolano B., 2012, A&A, 539, A148
Bitsch B., Lambrechts M., Johansen A., 2015, A&A, 582, A112
Blum J., Wurm G., 2008, ARA&A, 46, 21
Boley A. C., Durisen R. H., 2010, ApJ, 724, 618
Boss A. P., 2000, ApJ, 536, L101
Brewer J. M., Fischer D. A., Madhusudhan N., 2017, AJ, 153, 83
Brickhouse N. S., Cranmer S. R., Dupree A. K., Günther H. M., Luna G. J. M., Wolk S. J., 2012, ApJ, 760, L21
Ciesla F. J., Cuzzi J. N., 2006, Icarus, 181, 178
Clarke C. J., Lodato G., 2009, MNRAS, 398, L6
Collings M. P., Anderson M. A., Chen R., Dever J. W., Viti S., Williams D. A., McCoustra M. R. S., 2004, MNRAS, 354, 1133
Crida A., Morbidelli A., 2007, MNRAS, 377, 1324
Cridland A. J., Pudritz R. E., Alessi M., 2016, MNRAS, 461, 3274
Cridland A. J., Pudritz R. E., Birnstiel T., 2017, MNRAS, 465, 3865
Currie T., Lada C. J., Plavchan P., Robitaille T. P., Irwin J., Kenyon S. J., 2009, ApJ, 698, 1
Draine B. T., 2003, ARA&A, 41, 241
Du F., Bergin E. A., Hogerheijde M. R., 2015, ApJ, 807, L32
Eistrup C., Walsh C., van Dishoeck E. F., 2016, A&A, 595, A83
Favre C., Cleeves L. I., Bergin E. A., Qi C., Blake G. A., 2013, ApJ, 776, L38
Fayolle E. C., Balfe J., Loomis R., Bergner J., Graninger D., Rajappan M., Öberg K. I., 2016, ApJ, 816, L28
Fedele D., van den Ancker M. E., Henning T., Jayawardhana R., Oliveira J. M., 2010, A&A, 510, A72
Forgan D., Rice K., 2011, MNRAS, 417, 1928
Garaud P., 2007, ApJ, 671, 2091
Garrod R. T., Herbst E., 2006, A&A, 457, 927
Guillot T., Hueso R., 2006, MNRAS, 367, L47
Guilloteau S., Dutrey A., Piétu V., Boehler Y., 2011, A&A, 529, A105
Gundlach B., Blum J., 2015, ApJ, 798, 34
Haisch K. E., Jr, Lada E. A. Lada C. J., 2001, ApJ, 553, L153
Haynes K., Mandell A. M., Madhusudhan N., Deming D., Knutson H., 2015, ApJ, 806, 146
Helled R., Lunine J., 2014, MNRAS, 441, 2273
Hollenbach D., Kaufman M. J., Bergin E. A., Melnick G. J., 2009, ApJ, 690, 1497
Hueso R., Guillot T., 2003, Space Sci. Rev., 106, 105
Hueso R., Guillot T., 2005, A&A, 442, 703
Kama M., Folsom C. P., Pinilla P., 2015, A&A, 582, L10
Kama M. et al., 2016, A&A, 588, A108
Kobayashi H., Tanaka H., Krivov A. V., 2011, ApJ, 738, 35
Kóspál Á. et al., 2013, ApJ, 776, 77
Kozai Y., 1962, AJ, 67, 591
Kreidberg L. et al., 2014, ApJ, 793, L27
Kreidberg L. et al., 2015, ApJ, 814, 66
Laibe G., Price D. J., 2014, MNRAS, 444, 1940
Lambrechts M., Johansen A., 2012, A&A, 544, A32
Lambrechts M., Johansen A., 2014, A&A, 572, A107
Lambrechts M., Johansen A., Morbidelli A., 2014, A&A, 572, A35
Lega E., Morbidelli A., Nesvorný D., 2013, MNRAS, 431, 3494
Lidov M. L., 1962, Planet. Space Sci., 9, 719
Line M. R., Knutson H., Wolf A. S., Yung Y. L., 2014, ApJ, 783, 70
Lodders K., 2004, ApJ, 611, 587
Lodders K., Fegley B., 2002, Icarus, 155, 393
Lommen D. et al., 2007, A&A, 462, 211
Lynden-Bell D., Pringle J. E., 1974, MNRAS, 168, 603
Machida M. N., Kokubo E., Inutsuka S.-I., Matsumoto T., 2010, MNRAS, 405, 1227
Madhusudhan N., 2012, ApJ, 758, 36
Madhusudhan N., Mousis O., Johnson T. V., Lunine J. I., 2011, ApJ, 743, 191

Madhusudhan N., Crouzet N., McCullough P. R., Deming D., Hedges C., 2014a, ApJ, 791, L9

Madhusudhan N., Amin M. A., Kennedy G. M., 2014b, ApJ, 794, L12

Madhusudhan N., Bitsch B., Johansen A., Eriksson L., 2016, MNRAS, preprint (arXiv:1611.03083)

Manara C. F. et al., 2016, A&A, 591, L3

Mathis J. S., Rumpl W., Nordsieck K. H., 1977, ApJ, 217, 425

Matousek S., 2007, Acta Astronaut., 61, 932

Matrà L., Panić O., Wyatt M. C., Dent W. R. F., 2015, MNRAS, 447, 3936

Meng H. Y. A., Rieke G. H., Su K. Y. L., Gaspar A., 2017, ApJ, 836, 34

Monga N., Desch S., 2015, ApJ, 798, 9

Mordasini C., Mollière P., Dittkrist K.-M., Jin S., Alibert Y., 2015, Int. J. Astrobiol., 14, 201

Moses J. I. et al., 2013, ApJ, 777, 34

Öberg K. I., Bergin E. A., 2016, ApJ, 831, L19

Öberg K. I., Murray-Clay R., Bergin E. A., 2011, ApJ, 743, L16

Ormel C. W., Klahr H. H., 2010, A&A, 520, A43

Owen T., Mahaffy P., Niemann H. B., Atreya S., Donahue T., Bar-Nun A., de Pater I., 1999, Nature, 402, 269

Paardekooper S.-J., Baruteau C., Kley W., 2011, MNRAS, 410, 293

Pérez L. M. et al., 2012, ApJ, 760, L17

Pericaud J., Di Folco E., Dutrey A., Guilloteau S., Pietu V., 2017, A&A, 600, A62

Piétu V., Guilloteau S., Di Folco E., Dutrey A., Boehler Y., 2014, A&A, 564, A95

Pinhas A., Madhusudhan N., Clarke C., 2016, MNRAS, 463, 4516

Piso A.-M. A., Youdin A. N., 2014, ApJ, 786, 21

Pollack J. B., Hubickyj O., Bodenheimer P., Lissauer J. J., Podolak M., Greenzweig Y., 1996, Icarus, 124, 62

Pontoppidan K. M., 2006, A&A, 453, L47

Raymond S. N., Quinn T., Lunine J. I., 2006, Icarus, 183, 265

Raymond S. N., Kokubo E., Morbidelli A., Morishima R., Walsh K. J., 2014, Protostars and Planets VI. Univ. Arizona Press, Tucson, p. 595

Rice W. K. M., Armitage P. J., 2009, MNRAS, 396, 2228

Rodmann J., Henning T., Chandler C. J., Mundy L. G., Wilner D. J., 2006, A&A, 446, 211

Rosotti G. P., Juhasz A., Booth R. A., Clarke C. J., 2016, MNRAS, 459, 2790

Saito E., Sirono S.-i., 2011, ApJ, 728, 20

Schoonenberg D., Ormel C. W., 2017, A&A, 602, A21

Stammler S. M., Birnstiel T., Panić O., Dullemond C. P., Dominik C., 2017, A&A, 600, A140

Stepinski T. F., Valageas P., 1997, A&A, 319, 1007

Stevenson K. B., Bean J. L., Seifahrt A., Désert J.-M., Madhusudhan N., Bergmann M., Kreidberg L., Homeier D., 2014, AJ, 147, 161

Tanaka H., Himeno Y., Ida S., 2005, ApJ, 625, 414

Tazzari M. et al., 2016, A&A, 588, A53

Thi W.-F. et al., 2014, A&A, 561, A50

Tsai S.-M., Lyons J. R., Grosheintz L., Rimmer P. B., Kitzmann D., Heng K., 2017, ApJS, 228, 20

Tsiganis K., Gomes R., Morbidelli A., Levison H. F., 2005, Nature, 435, 459

Visscher C., Moses J. I., Saslow S. A., 2010, Icarus, 209, 602

Visser R., 2009, PhD thesis, Univ. Leiden, Leiden

Walsh K. J., Morbidelli A., Raymond S. N., O'Brien D. P., Mandell A. M., 2011, Nature, 475, 206

Wilner D. J., D'Alessio P., Calvet N., Claussen M. J., Hartmann L., 2005, ApJ, 626, L109

Wilson H. F., Militzer B., 2012, Phys. Rev. Lett., 108, 111101

Woitke P., Kamp I., Thi W.-F., 2009, A&A, 501, 383

Wyatt M. C., Panić O., Kennedy G. M., Matrà L., 2015, Ap&SS, 357, 103

Youdin A. N., Lithwick Y., 2007, Icarus, 192, 588

Zhu Z., Hartmann L., Nelson R. P., Gammie C. F., 2012, ApJ, 746, 110

This paper has been typeset from a TEX/LATEX file prepared by the author.